

# Branching Ratio and CP Asymmetry of $B \rightarrow \rho\eta^{(\prime)}$ Decays in the Perturbative QCD Approach

Xin Liu, Huisheng Wang, Zhenjun Xiao,<sup>\*</sup> and Libo Guo<sup>†</sup>

*Department of Physics and Institute of Theoretical Physics ,  
Nanjing Normal University, Nanjing, Jiangsu 210097, P.R.China*

Cai-Dian Lü

*CCAST (World Laboratory), P.O. Box 8730, Beijing 100080, China; and*

*Institute of High Energy Physics, CAS,  
P.O. Box 918(4) Beijing 100049, China<sup>‡</sup>*

(Dated: June 24, 2018)

## Abstract

In this paper, we calculate the branching ratios and CP-violating asymmetries for  $B^0 \rightarrow \rho^0\eta^{(\prime)}$  and  $B^+ \rightarrow \rho^+\eta^{(\prime)}$  decays in the perturbative QCD factorization approach. In this approach, we not only calculate the usual factorizable contributions, but also evaluate the non-factorizable and annihilation type contributions. Besides the current-current operators, the contributions from the QCD and electroweak penguin operators are also taken into account. The theoretical predictions for the branching ratios are  $Br(B^+ \rightarrow \rho^+\eta^{(\prime)}) \approx 9 \times 10^{-6}$  and  $Br(B^0 \rightarrow \rho^0\eta^{(\prime)}) \approx 5 \times 10^{-8}$ , which agree well with the measured values and currently available experimental upper limits. We also predict large CP-violating asymmetries in these decays:  $A_{CP}^{dir}(\rho^\pm\eta) \approx -13\%$ ,  $A_{CP}^{dir}(\rho^\pm\eta') \approx -18\%$ ,  $A_{CP}^{dir}(\rho^0\eta) \approx -41\%$ ,  $A_{CP}^{dir}(\rho^0\eta') \approx -27\%$ ,  $A_{CP}^{mix}(\rho^0\eta) \approx +25\%$ , and  $A_{CP}^{mix}(\rho^0\eta') \approx +11\%$ , which can be tested by the current or future B factory experiments.

PACS numbers: 13.25.Hw, 12.38.Bx, 14.40.Nd

---

<sup>‡</sup> Mailing address.

<sup>\*</sup>Electronic address: xiaozhenjun@njnu.edu.cn

<sup>†</sup>Electronic address: guolb@email.njnu.edu.cn

## I. INTRODUCTION

Along with the great progress in theoretical studies and experimental measurements, the charmless two-body B meson decays are getting more and more interesting and attracting more and more attentions, since they provide a good place for testing the standard model (SM), studying CP violation and searching for possible new physics beyond the SM.

For the two-body hadronic B meson decays, the dominant theoretical error comes from the uncertainty in evaluating the hadronic matrix element  $\langle M_1 M_2 | O_i | B \rangle$  where  $M_1$  and  $M_2$  are light final mesons. At present, the QCD factorization (QCDF) approach [1, 2] and the perturbative QCD (PQCD) factorization approach [3, 4, 5] are the two popular methods being used to calculate the hadronic matrix elements. The perturbative QCD approach has been developed earlier from the QCD hard-scattering approach [3]. Some elements of this approach are also present in the QCD factorization formula of Refs. [1, 2]. The two major differences between these two approaches are (a) the form factors are calculable perturbatively in PQCD approach, but taken as the input parameters extracted from other experimental measurements in the QCDF approach; and (b) the annihilation contributions are calculable and play an important role in producing CP violation for the considered decay modes in PQCD approach, but it could not be evaluated reliably in QCDF approach. Of course, one should remember that the assumptions behind the PQCD approach, specifically the possibility to calculate the form factors perturbatively, are still under discussion [6]. More efforts are needed to clarify these problems.

Up to now, many B meson hadronic decay channels have been calculated and studied phenomenologically in both the QCDF approach [1, 7, 8] and in the PQCD approach [9, 10, 11, 12, 13]. In this paper, we would like to calculate the branching ratios and CP asymmetries for the  $B \rightarrow \rho \eta^{(\prime)}$  decays by employing the low energy effective Hamiltonian [14] and the PQCD approach. Besides the usual factorizable contributions, we here are able to evaluate the non-factorizable and the annihilation contributions to these decays.

Theoretically, the four  $B \rightarrow \rho \eta^{(\prime)}$  decays have been studied before in the naive or generalized factorization approach [15], as well as in the QCD factorization approach [8]. On the experimental side, the branching ratios of  $B \rightarrow \rho^+ \eta, \rho^+ \eta'$  decays have been measured [16, 17, 18, 19],

$$\begin{aligned} Br(B^+ \rightarrow \rho^+ \eta) &= (8.1_{-1.5}^{+1.7}) \times 10^{-6}, \\ Br(B^+ \rightarrow \rho^+ \eta') &= (12.9_{-5.5}^{+6.2} \pm 2.0) \times 10^{-6}. \end{aligned} \quad (1)$$

For  $B \rightarrow \rho^0 \eta, \rho^0 \eta'$  decays, only the experimental upper limits are available now [19]

$$Br(B^0 \rightarrow \rho^0 \eta) < 1.5 \times 10^{-6}, \quad Br(B^0 \rightarrow \rho^0 \eta') < 4.3 \times 10^{-6}. \quad (2)$$

In  $B \rightarrow \rho \eta^{(\prime)}$  decays, the B meson is heavy, setting at rest and decaying into two light mesons (i.e.  $\rho$  and  $\eta^{(\prime)}$ ) with large momenta. Therefore the light final state mesons are moving very fast in the rest frame of B meson. In this case, the short distance hard process dominates the decay amplitude. We assume that the soft final state interaction is not important for such decays, since there is not enough time for light mesons to exchange soft gluons. Therefore, it makes the PQCD reliable in calculating the  $B \rightarrow \rho \eta^{(\prime)}$  decays. With the Sudakov resummation, we can include the leading double logarithms for all

loop diagrams, in association with the soft contribution. Unlike the usual factorization approach, the hard part of the PQCD approach consists of six quarks rather than four. We thus call it six-quark operators or six-quark effective theory. Applying the six-quark effective theory to  $B$  meson decays, we need meson wave functions for the hadronization of quarks into mesons. All the collinear dynamics are included in the meson wave functions.

This paper is organized as follows. In Sec. II, we give a brief review for the PQCD factorization approach. In Sec. III, we calculate analytically the related Feynman diagrams and present the various decay amplitudes for the studied decay modes. In Sec. IV, we show the numerical results for the branching ratios and CP asymmetries of  $B \rightarrow \rho\eta^{(\prime)}$  decays and comparing them with the measured values. The summary and some discussions are included in the final section.

## II. THEORETICAL FRAMEWORK

The three scale PQCD factorization approach has been developed and applied in the non-leptonic  $B$  meson decays [3, 4, 5, 9, 10, 11, 12] for some time. In this approach, the decay amplitude is separated into soft, hard, and harder dynamics characterized by different energy scales ( $t, m_b, M_W$ ). It is conceptually written as the convolution,

$$\mathcal{A}(B \rightarrow M_1 M_2) \sim \int d^4 k_1 d^4 k_2 d^4 k_3 \text{Tr} [C(t) \Phi_B(k_1) \Phi_{M_1}(k_2) \Phi_{M_2}(k_3) H(k_1, k_2, k_3, t)], \quad (3)$$

where  $k_i$ 's are momenta of light quarks included in each mesons, and Tr denotes the trace over Dirac and color indices.  $C(t)$  is the Wilson coefficient which results from the radiative corrections at short distance. In the above convolution,  $C(t)$  includes the harder dynamics at larger scale than  $M_B$  scale and describes the evolution of local 4-Fermi operators from  $m_W$  (the  $W$  boson mass) down to  $t \sim \mathcal{O}(\sqrt{\bar{\Lambda} M_B})$  scale, where  $\bar{\Lambda} \equiv M_B - m_b$ . The function  $H(k_1, k_2, k_3, t)$  describes the four quark operator and the spectator quark connected by a hard gluon whose  $q^2$  is in the order of  $\bar{\Lambda} M_B$ , and includes the  $\mathcal{O}(\sqrt{\bar{\Lambda} M_B})$  hard dynamics. Therefore, this hard part  $H$  can be perturbatively calculated. The function  $\Phi_M$  is the wave function which describes hadronization of the quark and anti-quark to the meson  $M$ . While the function  $H$  depends on the processes considered, the wave function  $\Phi_M$  is independent of the specific processes. Using the wave functions determined from other well measured processes, one can make quantitative predictions here.

Since the  $b$  quark is rather heavy we consider the  $B$  meson at rest for simplicity. It is convenient to use light-cone coordinate  $(p^+, p^-, \mathbf{p}_T)$  to describe the meson's momenta,

$$p^\pm = \frac{1}{\sqrt{2}}(p^0 \pm p^3), \quad \text{and} \quad \mathbf{p}_T = (p^1, p^2). \quad (4)$$

Through out this paper, we use the light-cone coordinates to write the four momentum as  $(k_1^+, k_1^-, k_1^\perp)$ . Using these coordinates the  $B$  meson and the two final state meson momenta can be written as

$$P_1 = \frac{M_B}{\sqrt{2}}(1, 1, \mathbf{0}_T), \quad P_2 = \frac{M_B}{\sqrt{2}}(1, r_\rho^2, \mathbf{0}_T), \quad P_3 = \frac{M_B}{\sqrt{2}}(0, 1, \mathbf{0}_T), \quad (5)$$

respectively, where  $r_\rho = m_\rho/m_B$ ; the light pseudoscalar meson masses have been neglected.

For the  $B \rightarrow \rho\eta^{(\prime)}$  decays considered here, only the  $\rho$  meson's longitudinal part contributes to the decays, its polar vector is  $\epsilon_L = \frac{M_B}{\sqrt{2}M_\rho}(1, -r_\rho^2, \mathbf{0}_T)$ . Putting the light (anti-) quark momenta in  $B$ ,  $\rho$  and  $\eta^{(\prime)}$  mesons as  $k_1$ ,  $k_2$ , and  $k_3$ , respectively, we can choose

$$k_1 = (x_1 P_1^+, 0, \mathbf{k}_{1T}), \quad k_2 = (x_2 P_2^+, 0, \mathbf{k}_{2T}), \quad k_3 = (0, x_3 P_3^-, \mathbf{k}_{3T}). \quad (6)$$

Then, the integration over  $k_1^-$ ,  $k_2^-$ , and  $k_3^+$  in eq.(3) will lead to

$$\mathcal{A}(B \rightarrow \rho\eta^{(\prime)}) \sim \int dx_1 dx_2 dx_3 b_1 db_1 b_2 db_2 b_3 db_3 \text{Tr} \left[ C(t) \Phi_B(x_1, b_1) \Phi_\rho(x_2, b_2) \Phi_{\eta^{(\prime)}}(x_3, b_3) H(x_i, b_i, t) S_t(x_i) e^{-S(t)} \right], \quad (7)$$

where  $b_i$  is the conjugate space coordinate of  $k_{iT}$ , and  $t$  is the largest energy scale in function  $H(x_i, b_i, t)$ . The large logarithms ( $\ln \frac{m_W}{t}$ ) coming from QCD radiative corrections to four quark operators are included in the Wilson coefficients  $C(t)$ . The large double logarithms ( $\ln^2 x_i$ ) on the longitudinal direction are summed by the threshold resummation [20], and they lead to  $S_t(x_i)$  which smears the end-point singularities on  $x_i$ . The last term,  $e^{-S(t)}$ , is the Sudakov form factor resulting from overlap of soft and collinear divergences, which suppresses the soft dynamics effectively [21]. Thus it makes the perturbative calculation of the hard part  $H$  applicable at intermediate scale, i.e.,  $M_B$  scale. We will calculate analytically the function  $H(x_i, b_i, t)$  for  $B \rightarrow \rho\eta^{(\prime)}$  decays in the first order in  $\alpha_s$  expansion and give the convoluted amplitudes in next section.

### A. Wilson coefficients

For  $B \rightarrow \rho\eta^{(\prime)}$  decays, the related weak effective Hamiltonian  $\mathcal{H}_{eff}$  can be written as [14]

$$\mathcal{H}_{eff} = \frac{G_F}{\sqrt{2}} \left[ V_{ub} V_{ud}^* (C_1(\mu) O_1^u(\mu) + C_2(\mu) O_2^u(\mu)) - V_{tb} V_{td}^* \sum_{i=3}^{10} C_i(\mu) O_i(\mu) \right]. \quad (8)$$

We specify below the operators in  $\mathcal{H}_{eff}$  for  $b \rightarrow d$  transition:

$$\begin{aligned} O_1^u &= \bar{d}_\alpha \gamma^\mu L u_\beta \cdot \bar{u}_\beta \gamma_\mu L b_\alpha, & O_2^u &= \bar{d}_\alpha \gamma^\mu L u_\alpha \cdot \bar{u}_\beta \gamma_\mu L b_\beta, \\ O_3 &= \bar{d}_\alpha \gamma^\mu L b_\alpha \cdot \sum_{q'} \bar{q}'_\beta \gamma_\mu L q'_\beta, & O_4 &= \bar{d}_\alpha \gamma^\mu L b_\beta \cdot \sum_{q'} \bar{q}'_\beta \gamma_\mu L q'_\alpha, \\ O_5 &= \bar{d}_\alpha \gamma^\mu L b_\alpha \cdot \sum_{q'} \bar{q}'_\beta \gamma_\mu R q'_\beta, & O_6 &= \bar{d}_\alpha \gamma^\mu L b_\beta \cdot \sum_{q'} \bar{q}'_\beta \gamma_\mu R q'_\alpha, \\ O_7 &= \frac{3}{2} \bar{d}_\alpha \gamma^\mu L b_\alpha \cdot \sum_{q'} e_{q'} \bar{q}'_\beta \gamma_\mu R q'_\beta, & O_8 &= \frac{3}{2} \bar{d}_\alpha \gamma^\mu L b_\beta \cdot \sum_{q'} e_{q'} \bar{q}'_\beta \gamma_\mu R q'_\alpha, \\ O_9 &= \frac{3}{2} \bar{d}_\alpha \gamma^\mu L b_\alpha \cdot \sum_{q'} e_{q'} \bar{q}'_\beta \gamma_\mu L q'_\beta, & O_{10} &= \frac{3}{2} \bar{d}_\alpha \gamma^\mu L b_\beta \cdot \sum_{q'} e_{q'} \bar{q}'_\beta \gamma_\mu L q'_\alpha, \end{aligned} \quad (9)$$

where  $\alpha$  and  $\beta$  are the  $SU(3)$  color indices;  $L$  and  $R$  are the left- and right-handed projection operators with  $L = (1 - \gamma_5)$ ,  $R = (1 + \gamma_5)$ . The sum over  $q'$  runs over the quark fields that are active at the scale  $\mu = O(m_b)$ , i.e., ( $q' \in \{u, d, s, c, b\}$ ). The PQCD approach works well for the leading twist approximation and leading double logarithm summation. For the Wilson coefficients  $C_i(\mu)$  ( $i = 1, \dots, 10$ ), we will also use the leading order (LO) expressions, although the next-to-leading order calculations already exist in the literature [14]. This is the consistent way to cancel the explicit  $\mu$  dependence in the theoretical formulae.

For the renormalization group evolution of the Wilson coefficients from higher scale to lower scale, we use the formulae as given in Ref.[9] directly. At the high  $m_W$  scale, the leading order Wilson coefficients  $C_i(M_W)$  are simple and can be found easily in Ref.[14].

In PQCD approach, the scale  $t$  is chosen at the maximum value of various subprocess scales to suppress the higher order corrections, which may be larger or smaller than the  $m_b$  scale. In the range of  $m_b \leq t < m_W$ , we will evaluate the Wilson coefficients  $C_i(t)$  at scale  $t$  by using the leading logarithm running equations, as given explicitly in Eq.(C1) of Ref. [9]. In numerical calculations, we also use  $\alpha_s = 4\pi/[\beta_1 \ln(t^2/\Lambda_{QCD}^{(5)})^2]$  which is the leading order expression with  $\Lambda_{QCD}^{(5)} = 193\text{MeV}$ , derived from  $\Lambda_{QCD}^{(4)} = 250\text{MeV}$ . Here  $\beta_1 = (33 - 2n_f)/12$ , with the appropriate number of active quarks  $n_f$ :  $n_f = 5$  for  $t \geq m_b$ .

At a given energy scale  $t = m_b = 4.8 \text{ GeV}$ , the LO Wilson coefficients  $C_i(m_b)$  as given in Ref. [9] are

$$\begin{aligned} C_1 &= -0.2703, & C_2 &= 1.1188, & C_3 &= 0.0126, & C_4 &= -0.0270, \\ C_5 &= 0.0085, & C_6 &= -0.0326, & C_7 &= 0.0011, & C_8 &= 0.0004, \\ C_9 &= -0.0090, & C_{10} &= 0.0022. \end{aligned} \quad (10)$$

In the range of  $t < m_b$ , then we evaluate the Wilson coefficients  $C_i(t)$  by using the  $C_i(m_b)$  in Eq. (10) as boundary input and the leading logarithmic running equations as given in Appendix D of Ref. [9] for the case of  $n_f = 4$ . For the Wilson coefficient  $C_2(t)$ , for example, the running equation in the two different regions can be written as

$$C_2(t) = \frac{1}{2} (\eta^{-6/23} + \eta^{2/23}), \quad \text{for } m_b \leq t < m_W, \quad (11)$$

$$\begin{aligned} C_2(t) &= \frac{1}{4} (\eta^{-6/23} + \eta^{2/23}) (\xi^{-6/25} + \xi^{12/25}) \\ &\quad + \frac{1}{4} (\eta^{-6/23} - \eta^{2/23}) (\xi^{-6/25} - \xi^{12/25}), \quad \text{for } t < m_b, \end{aligned} \quad (12)$$

where  $\eta = \alpha_S(t)/\alpha_S(m_W)$  and  $\xi = \alpha_S(t)/\alpha_S(m_b)$ . For the running equations of other Wilson coefficients one can see Appendix C and D of ref. [9].

## B. Wave Functions

In the resummation procedures, the  $B$  meson is treated as a heavy-light system. In general, the  $B$  meson light-cone matrix element can be decomposed as [7, 22]

$$\begin{aligned} &\int_0^1 \frac{d^4 z}{(2\pi)^4} e^{i\mathbf{k}_1 \cdot \mathbf{z}} \langle 0 | \bar{b}_\alpha(0) d_\beta(z) | B(p_B) \rangle \\ &= -\frac{i}{\sqrt{2N_c}} \left\{ (\not{p}_B + m_B) \gamma_5 \left[ \phi_B(\mathbf{k}_1) - \frac{\not{n} - \not{v}}{\sqrt{2}} \bar{\phi}_B(\mathbf{k}_1) \right] \right\}_{\beta\alpha}, \end{aligned} \quad (13)$$

where  $n = (1, 0, \mathbf{0}_T)$ , and  $v = (0, 1, \mathbf{0}_T)$  are the unit vectors pointing to the plus and minus directions, respectively. From the above equation, one can see that there are two Lorentz structures in the  $B$  meson distribution amplitudes. They obey to the following normalization conditions

$$\int \frac{d^4 k_1}{(2\pi)^4} \phi_B(\mathbf{k}_1) = \frac{f_B}{2\sqrt{2N_c}}, \quad \int \frac{d^4 k_1}{(2\pi)^4} \bar{\phi}_B(\mathbf{k}_1) = 0. \quad (14)$$

In general, one should consider these two Lorentz structures in calculations of  $B$  meson decays. However, it can be argued that the contribution of  $\bar{\phi}_B$  is numerically small [23], thus its contribution can be numerically neglected. Using this approximation, we can reduce one input parameter in our calculation. Therefore, we only consider the contribution of Lorentz structure

$$\Phi_B = \frac{1}{\sqrt{2N_c}}(\not{p}_B + m_B)\gamma_5\phi_B(\mathbf{k}_1). \quad (15)$$

In the next section, we will see that the hard part is always independent of one of the  $k_1^+$  and/or  $k_1^-$ , if we make approximations shown in next section. The  $B$  meson wave function is then the function of variable  $k_1^-$  (or  $k_1^+$ ) and  $k_1^\perp$ ,

$$\phi_B(k_1^-, k_1^\perp) = \int dk_1^+ \phi(k_1^+, k_1^-, k_1^\perp). \quad (16)$$

The wave function for  $d\bar{d}$  components in  $\eta^{(\prime)}$  meson are given as:

$$\Phi_{\eta_{d\bar{d}}}(P, x, \zeta) \equiv \frac{1}{\sqrt{2N_c}} \left\{ \not{p} \phi_{\eta_{d\bar{d}}}^A(x) + m_0^{\eta_{d\bar{d}}} \phi_{\eta_{d\bar{d}}}^P(x) + \zeta m_0^{\eta_{d\bar{d}}} (\not{p} \not{n} - v \cdot n) \phi_{\eta_{d\bar{d}}}^T(x) \right\} \quad (17)$$

where  $P$  and  $x$  are the momentum and the momentum fraction of  $\eta_{d\bar{d}}$ , respectively. We assumed here that the wave function of  $\eta_{d\bar{d}}$  is same as the  $\pi$  wave function. The parameter  $\zeta$  is either  $+1$  or  $-1$  depending on the assignment of the momentum fraction  $x$ .

In  $B \rightarrow \rho \eta^{(\prime)}$  decays,  $\rho$  meson is longitudinally polarized. We only consider its wave function in longitudinal polarization [23, 25],

$$\langle \rho^-(P, \epsilon_L) | \bar{d}_\alpha(z) u_\beta(0) | 0 \rangle = \frac{1}{\sqrt{2N_c}} \int_0^1 dx e^{ixP \cdot z} \left\{ \not{\epsilon} \left[ \not{p}_\rho \phi_\rho^t(x) + m_\rho \phi_\rho(x) \right] + m_\rho \phi_\rho^s(x) \right\} \quad (18)$$

The second term in above equation is the leading twist wave function (twist-2), while the first and third terms are sub-leading twist (twist-3) wave functions.

The transverse momentum  $k^\perp$  is usually conveniently converted to the  $b$  parameter by Fourier transformation. The initial conditions of leading twist  $\phi_i(x)$ ,  $i = B, \rho, \eta, \eta'$ , are of non-perturbative origin, satisfying the normalization

$$\int_0^1 \phi_i(x, b=0) dx = \frac{1}{2\sqrt{6}} f_i, \quad (19)$$

with  $f_i$  the meson decay constants.

### III. PERTURBATIVE CALCULATIONS

In the previous section we have discussed the wave functions and Wilson coefficients of the amplitude in eq.(3). In this section, we will calculate the hard part  $H(t)$ . This part involves the four quark operators and the necessary hard gluon connecting the four quark operator and the spectator quark. We will show the whole amplitude for each diagram including wave functions. Similar to the  $B \rightarrow \pi \rho$  decays [26], the eight diagrams

contributing to the  $B \rightarrow \rho \eta^{(\prime)}$  decays are shown in Figure 1. We first calculate the usual factorizable diagrams (a) and (b). Operators  $O_1, O_2, O_3, O_4, O_9$ , and  $O_{10}$  are  $(V - A)(V - A)$  currents, the sum of their amplitudes is given as

$$\begin{aligned}
F_{e\rho} = & 4\sqrt{2}G_F\pi C_F m_B^4 \int_0^1 dx_1 dx_3 \int_0^\infty b_1 db_1 b_3 db_3 \phi_B(x_1, b_1) \\
& \cdot \{ [(1+x_3)\phi_\rho(x_3, b_3) + (1-2x_3)r_\rho(\phi_\rho^s(x_3, b_3) + \phi_\rho^t(x_3, b_3))] \\
& \alpha_s(t_e^1)h_e(x_1, x_3, b_1, b_3) \exp[-S_{ab}(t_e^1)] \\
& + 2r_\rho\phi_\rho^s(x_3, b_3)\alpha_s(t_e^2)h_e(x_3, x_1, b_3, b_1) \exp[-S_{ab}(t_e^2)] \} , \quad (20)
\end{aligned}$$

where  $C_F = 4/3$  is a color factor. The explicit expressions of the functions  $h_e^i$ , the energy scales  $t_e^i$  and the Sudakov factors  $S_{ab}(t)$  Can be found in the Appendix. In the above equation, we do not include the Wilson coefficients of the corresponding operators, which are process dependent. They will be shown later in this section for different decay channels. The diagrams Fig. 1(a) and 1(b) are also the diagrams for the  $B \rightarrow \rho$  form factor  $A_0^{B \rightarrow \rho}$ . Therefore we can extract  $A_0^{B \rightarrow \rho}$  from Eq. (20).

The operators  $O_5, O_6, O_7$ , and  $O_8$  have a structure of  $(V - A)(V + A)$ . In some decay channels, some of these operators contribute to the decay amplitude in a factorizable way. Since only the axial-vector part of  $(V + A)$  current contribute to the pseudo-scalar meson production,

$$\langle \rho | V - A | B \rangle \langle \eta | V + A | 0 \rangle = -\langle \rho | V - A | B \rangle \langle \eta | V - A | 0 \rangle, \quad (21)$$

the result of these operators is opposite to Eq. (20). In some other cases, we need to do Fierz transformation for these operators to get right color structure for factorization to work. In this case, we get  $(S + P)(S - P)$  operators from  $(V - A)(V + A)$  ones. For these  $(S + P)(S - P)$  operators, Fig. 1(a) and 1(b) give

$$\begin{aligned}
F_{e\rho}^P = & 8\sqrt{2}G_F\pi C_F f_\eta^d m_B^4 \int_0^1 dx_1 dx_3 \int_0^\infty b_1 db_1 b_3 db_3 \phi_B(x_1, b_1) \\
& \cdot \{ [\phi_\rho(x_3, b_3) + r_\rho((x_3 + 2)\phi_\rho^s(x_3, b_3) - x_3\phi_\rho^t(x_3, b_3))] \\
& \cdot \alpha_s(t_e^1)h_e(x_1, x_3, b_1, b_3) \exp[-S_{ab}(t_e^1)] \\
& + (x_1\phi_\rho(x_3, b_3) + 2r_\rho\phi_\rho^s(x_3, b_3)) \alpha_s(t_e^2)h_e(x_3, x_1, b_3, b_1) \exp[-S_{ab}(t_e^2)] \} . \quad (22)
\end{aligned}$$

For the non-factorizable diagrams (c) and (d), all three meson wave functions are involved. The integration of  $b_3$  can be performed using  $\delta(b_3 - b_2)$ , leaving only integration of  $b_1$  and  $b_2$ . For the  $(V - A)(V - A)$  operators, the result is

$$\begin{aligned}
M_{e\rho} = & -\frac{16}{\sqrt{3}}G_F\pi C_F m_B^4 \int_0^1 dx_1 dx_2 dx_3 \int_0^\infty b_1 db_1 b_2 db_2 \phi_B(x_1, b_1) \phi_\eta^A(x_2, b_2) \\
& \cdot \{ x_3 [\phi_\rho(x_3, b_2) - 2r_\rho\phi_\rho^t(x_3, b_3)] \alpha_s(t_f)h_f(x_1, x_2, x_3, b_1, b_2) \exp[-S_{cd}(t_f)] \} . \quad (23)
\end{aligned}$$

For the non-factorizable annihilation diagrams (e) and (f), again all three wave functions are involved. Here we have two kinds of contributions.  $M_{a\rho}$  is the contribution

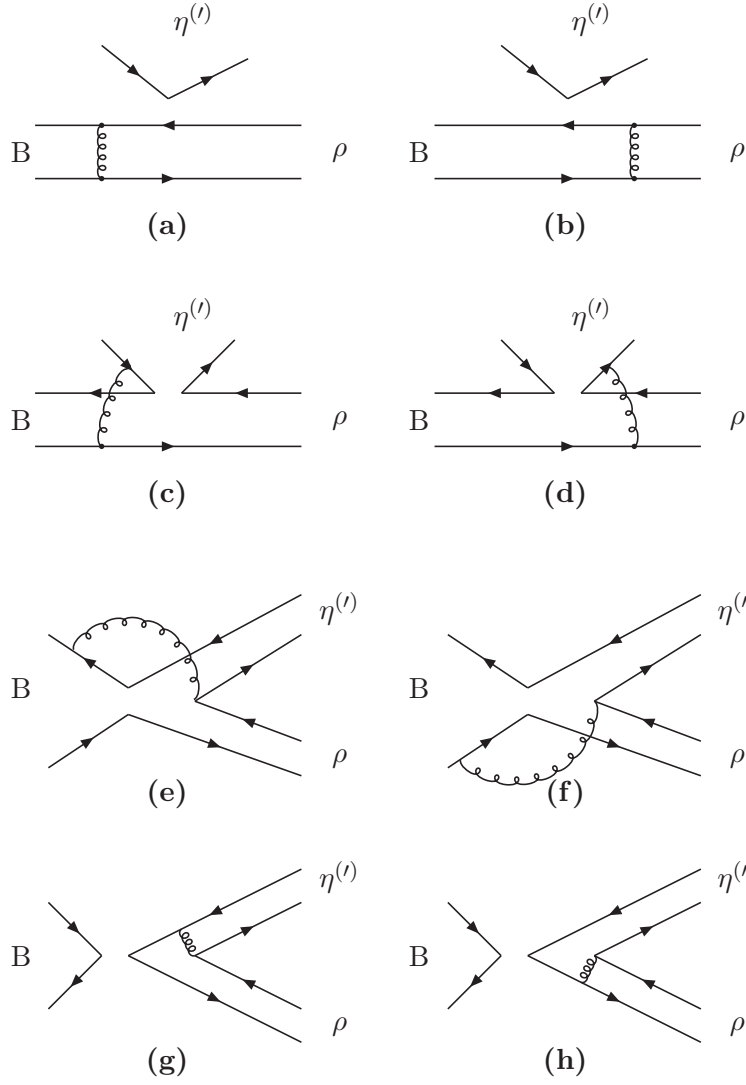


FIG. 1: Diagrams contributing to the  $B \rightarrow \rho \eta^{(l)}$  decays (diagram (a) and (b) contribute to the  $B \rightarrow \rho$  form factor  $A_0^{B \rightarrow \rho}$ ).

containing operator type  $(V - A)(V - A)$ , while  $M_{a\rho}^P$  is the contribution containing operator type  $(V - A)(V + A)$ .

$$\begin{aligned}
M_{a\rho} = & \frac{16}{\sqrt{3}} G_F \pi C_F m_B^4 \int_0^1 dx_1 dx_2 dx_3 \int_0^\infty b_1 db_1 b_2 db_2 \phi_B(x_1, b_1) \\
& \cdot \left\{ \left[ x_3 \phi_\rho(x_3, b_2) \phi_\eta^A(x_2, b_2) + r_\rho r_\eta \left( (x_3 - x_2) \left( \phi_\eta^P(x_2, b_2) \phi_\rho^t(x_3, b_2) + \phi_\eta^T(x_2, b_2) \right. \right. \right. \right. \\
& \cdot \phi_\rho^s(x_3, b_2) \left. \left. \left. \right) + (x_3 + x_2) \left( \phi_\eta^P(x_2, b_2) \phi_\rho^s(x_3, b_2) + \phi_\eta^T(x_2, b_2) \phi_\rho^t(x_3, b_2) \right) \right) \right] \\
& \cdot \alpha_s(t_f^1) h_f^1(x_1, x_2, x_3, b_1, b_2) \exp[-S_{ef}(t_f^1)] - \left[ x_2 \phi_\rho(x_3, b_2) \phi_\eta^A(x_2, b_2) \right. \\
& + r_\rho r_\eta \left( (x_2 - x_3) \left( \phi_\eta^P(x_2, b_2) \phi_\rho^t(x_3, b_2) + \phi_\eta^T(x_2, b_2) \phi_\rho^s(x_3, b_2) \right) + r_\rho r_\eta \right. \\
& \cdot \left. \left. \left. \left( (2 + x_2 + x_3) \phi_\eta^P(x_2, b_2) \phi_\rho^s(x_3, b_2) - (2 - x_2 - x_3) \phi_\eta^T(x_2, b_2) \phi_\rho^t(x_3, b_2) \right) \right) \right] \right. \\
& \cdot \left. \left. \alpha_s(t_f^2) h_f^2(x_1, x_2, x_3, b_1, b_2) \exp[-S_{ef}(t_f^2)] \right\} , \tag{24}
\end{aligned}$$

where  $r_\eta \equiv r_\pi = m_0^\pi/m_B$ .

$$\begin{aligned}
M_{a\rho}^P = & -\frac{16}{\sqrt{3}}G_F\pi C_F m_B^4 \int_0^1 dx_1 dx_2 dx_3 \int_0^\infty b_1 db_1 b_2 db_2 \phi_B(x_1, b_1) \\
& \cdot \{ [x_2 r_\eta \phi_\rho(x_3, b_2) (\phi_\eta^P(x_2, b_2) + \phi_\eta^T(x_2, b_2)) - x_3 r_\rho (\phi_\rho^s(x_3, b_2) + \phi_\rho^t(x_3, b_2)) \\
& \cdot \phi_\eta^A(x_2, b_2)] \alpha_s(t_f^1) h_f^1(x_1, x_2, x_3, b_1, b_2) \exp[-S_{ef}(t_f^1)] \\
& + [(2-x_2)r_\eta \phi_\rho(x_3, b_2) (\phi_\eta^P(x_2, b_2) + \phi_\eta^T(x_2, b_2)) - (2-x_3)r_\rho (\phi_\rho^s(x_3, b_2) \\
& + \phi_\rho^t(x_3, b_2)) \phi_\eta^A(x_2, b_2)] \alpha_s(t_f^2) h_f^2(x_1, x_2, x_3, b_1, b_2) \exp[-S_{ef}(t_f^2)] \} . \quad (25)
\end{aligned}$$

The factorizable annihilation diagrams (g) and (h) involve only  $\rho$  and  $\eta^{(\prime)}$  wave functions. There are also two kinds of decay amplitudes for these two diagrams.  $F_{a\rho}$  is for  $(V-A)(V-A)$  type operators, and  $F_{a\rho}^P$  is for  $(S-P)(S+P)$  type operators,

$$\begin{aligned}
F_{a\rho} = & -4\sqrt{2}\pi G_F C_F f_B m_B^4 \int_0^1 dx_2 dx_3 \int_0^\infty b_2 db_2 b_3 db_3 \\
& \cdot \{ [x_3 \phi_\rho(x_3, b_3) \phi_\eta^A(x_2, b_2) + 2r_\rho r_\eta \phi_\eta^P(x_2, b_2) ((1+x_3)\phi_\rho^s(x_3, b_3) \\
& - (1-x_3)\phi_\rho^t(x_3, b_2))] \alpha_s(t_e^3) h_a(x_2, x_3, b_2, b_3) \exp[-S_{gh}(t_e^3)] \\
& + [x_2 \phi_\rho(x_3, b_3) \phi_\eta^A(x_2, b_2) + 2r_\rho r_\eta \phi_\rho^s(x_3, b_3) ((1+x_2)\phi_\eta^P(x_2, b_2) \\
& - (1-x_2)\phi_\eta^T(x_2, b_2))] \alpha_s(t_e^4) h_a(x_3, x_2, b_3, b_2) \exp[-S_{gh}(t_e^4)] \} , \quad (26)
\end{aligned}$$

$$\begin{aligned}
F_{a\rho}^P = & -8\sqrt{2}G_F\pi C_F m_B^4 f_B \int_0^1 dx_2 dx_3 \int_0^\infty b_2 db_2 b_3 db_3 \\
& \cdot \{ [2r_\eta \phi_\rho(x_3, b_3) \phi_\eta^P(x_2, b_2) + x_3 r_\rho (\phi_\rho^s(x_3, b_3) - \phi_\rho^t(x_3, b_2)) \phi_\eta^A(x_2, b_2)] \\
& \cdot \alpha_s(t_e^3) h_a(x_2, x_3, b_2, b_3) \exp[-S_{gh}(t_e^3)] \\
& + [2r_\rho \phi_\rho^s(x_3, b_3) \phi_\eta^A(x_2, b_2) + x_2 r_\eta (\phi_\eta^P(x_2, b_2) - \phi_\eta^T(x_2, b_2)) \phi_\rho(x_3, b_3)] \\
& \cdot \alpha_s(t_e^4) h_a(x_3, x_2, b_3, b_2) \exp[-S_{gh}(t_e^4)] \} . \quad (27)
\end{aligned}$$

In the above equations, we have assumed that  $x_1 \ll x_2, x_3$ . Since the light quark momentum fraction  $x_1$  in  $B$  meson is peaked at the small  $x_1$  region, while quark momentum fraction  $x_2$  of  $\eta^{(\prime)}$  is peaked around 0.5, this is not a bad approximation. The numerical results also show that this approximation makes very little difference in the final result. After using this approximation, all the diagrams are functions of  $k_1^- = x_1 m_B / \sqrt{2}$  of  $B$  meson only, independent of the variable of  $k_1^+$ . Therefore the integration of eq.(16) is performed safely.

If we exchange the  $\rho$  and  $\eta^{(\prime)}$  in Figure 1, the result will be different. Because this will switch the dominant contribution from  $B \rightarrow \rho$  form factor to  $B \rightarrow \eta^{(\prime)}$  form factors. The new diagrams are shown in Figure 2.

We firstly consider the factorizable diagrams Fig. 2(a) and 2(b). The decay amplitude

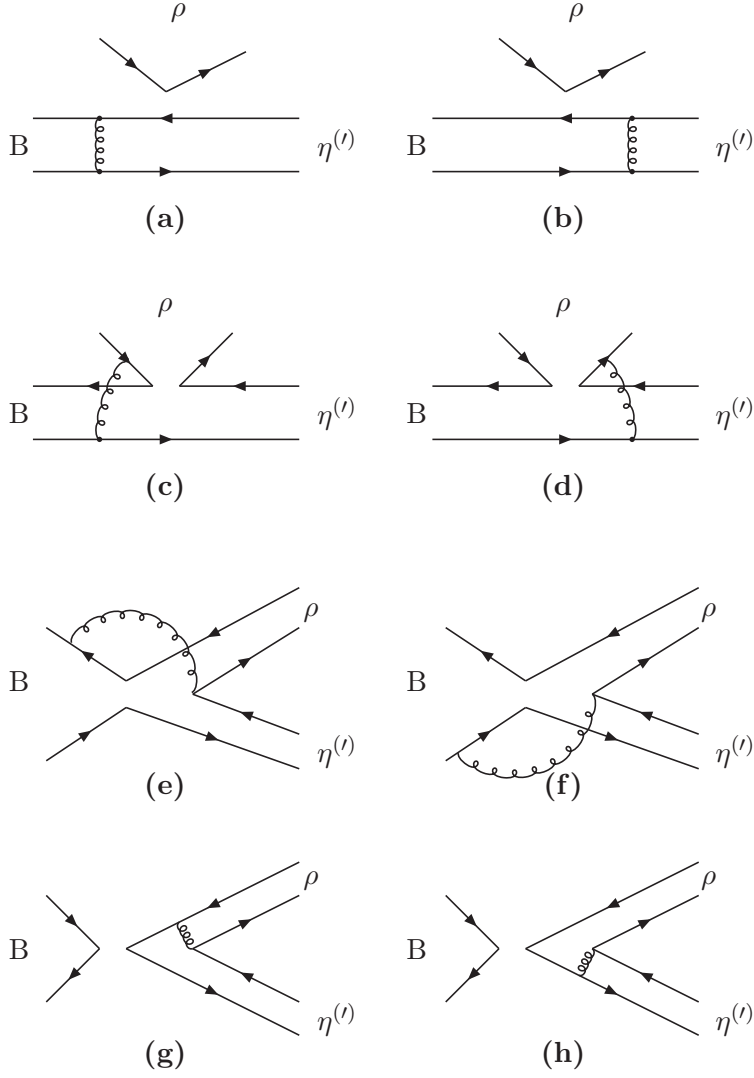


FIG. 2: Diagrams contributing to the  $B \rightarrow \rho\eta^{(\prime)}$  decays (diagram (a) and (b) contribute to the  $B \rightarrow \eta^{(\prime)}$  form factor  $F_0^{B \rightarrow \eta^{(\prime)}}$ ).

$F_e$  induced by inserting the  $(V - A)(V - A)$  operators is

$$\begin{aligned}
F_e = & 4\sqrt{2}\pi G_F C_F f_\rho m_B^4 \int_0^1 dx_1 dx_3 \int_0^\infty b_1 db_1 b_3 db_3 \phi_B(x_1, b_1) \\
& \cdot \left\{ \left[ (1 + x_3) \phi_\eta^A(x_3, b_3) + r_\eta (1 - 2x_3) (\phi_\eta^P(x_3, b_3) + \phi_\eta^T(x_3, b_3)) \right] \right. \\
& \cdot \alpha_s(t_e^1) h_e(x_1, x_3, b_1, b_3) \exp[-S_{ab}(t_e^1)] \\
& \left. + 2r_\eta \phi_\eta^P(x_3, b_3) \alpha_s(t_e^2) h_e(x_3, x_1, b_3, b_1) \exp[-S_{ab}(t_e^2)] \right\} . \quad (28)
\end{aligned}$$

These two diagrams are also responsible for the calculation of  $B \rightarrow \eta^{(\prime)}$  form factors  $F_0^{B \rightarrow \eta}$  and  $F_0^{B \rightarrow \eta'}$ , These two form factors can be extracted from Eq. (28).

Since only the vector part of the  $(V + A)$  current contribute to the vector meson production, the decay amplitude  $F_e^P$  induced by inserting  $(V - A)(V + A)$  operators is identical with the amplitude  $F_e$  as given in Eq. (28), i.e.,

$$F_e^P = F_e. \quad (29)$$

Because neither scalar nor pseudo-scalar density gives contribution to a vector meson production,  $\langle \rho | S + P | 0 \rangle = 0$ , we get  $F_e^{S+P} = 0$ .

For the non-factorizable diagrams Fig. 2(c) and 2(d), the corresponding decay amplitudes are

$$M_e = -\frac{16}{\sqrt{3}} G_F \pi C_F m_B^4 \int_0^1 dx_1 dx_2 dx_3 \int_0^\infty b_1 db_1 b_2 db_2 \phi_B(x_1, b_1) \phi_\rho(x_2, b_2) \cdot \{x_3 [\phi_\eta^A(x_3, b_2) - 2r_\eta \phi_\eta^T(x_3, b_2)] \alpha_s(t_f) h_f(x_1, x_2, x_3, b_1, b_2) \exp[-S_{cd}(t_f)]\} \quad (30)$$

$$M_e^P = -\frac{32}{\sqrt{3}} G_F \pi C_F r_\rho m_B^4 \int_0^1 dx_1 dx_2 dx_3 \int_0^\infty b_1 db_1 b_2 db_2 \phi_B(x_1, b_1) \cdot \{ [x_2 \phi_\eta^A(x_3, b_2) (\phi_\rho^s(x_2, b_2) - \phi_\rho^t(x_2, b_2)) + r_\eta ((x_2 + x_3) (\phi_\eta^P(x_3, b_2) \cdot \phi_\rho^s(x_2, b_2) + \phi_\eta^T(x_3, b_2) \phi_\rho^t(x_2, b_2)) + (x_3 - x_2) (\phi_\eta^P(x_3, b_2) \phi_\rho^t(x_2, b_2) + \phi_\eta^T(x_3, b_2) \phi_\rho^s(x_2, b_2)))] \alpha_s(t_f) h_f(x_1, x_2, x_3, b_1, b_2) \exp[-S_{cd}(t_f)] \} \quad (31)$$

From the non-factorizable annihilation diagrams Fig. 2(e) and 2(f), we find the decay amplitude  $M_a$  for  $(V - A)(V - A)$  operators,  $M_a^P$  for  $(V - A)(V + A)$  operators,

$$M_a = \frac{16}{\sqrt{3}} \pi G_F C_F m_B^4 \int_0^1 dx_1 dx_2 dx_3 \int_0^\infty b_1 db_1 b_2 db_2 \phi_B(x_1, b_1) \cdot \{ [x_3 \phi_\rho(x_2, b_2) \phi_\eta^A(x_3, b_2) + r_\rho r_\eta ((x_3 - x_2) (\phi_\eta^P(x_3, b_2) \phi_\rho^t(x_2, b_2) + \phi_\eta^T(x_3, b_2) \phi_\rho^s(x_2, b_2)) + (x_2 + x_3) (\phi_\eta^P(x_3, b_2) \phi_\rho^s(x_2, b_2) + \phi_\eta^T(x_3, b_2) \phi_\rho^t(x_2, b_2)))] \alpha_s(t_f^1) h_f^1(x_1, x_2, x_3, b_1, b_2) \exp[-S_{ef}(t_f^1)] + [x_2 \phi_\rho(x_2, b_2) \phi_\eta^A(x_3, b_2) + r_\rho r_\eta ((x_2 - x_3) (\phi_\eta^P(x_3, b_2) \phi_\rho^t(x_2, b_2) + \phi_\eta^T(x_3, b_2) \phi_\rho^s(x_2, b_2)) + (2 + x_2 + x_3) \phi_\eta^P(x_3, b_2) \phi_\rho^s(x_2, b_2) - (2 - x_2 - x_3) \phi_\eta^T(x_3, b_2) \phi_\rho^t(x_2, b_2))] \alpha_s(t_f^2) h_f^2(x_1, x_2, x_3, b_1, b_2) \exp[-S_{ef}(t_f^2)] \} \quad (32)$$

$$M_a^P = M_{a\rho}^P. \quad (33)$$

For the factorizable annihilation diagrams Fig. 2(g) and 2(h), we have

$$F_a = -F_{a\rho}, \quad \text{and} \quad F_a^P = -F_{a\rho}^P. \quad (34)$$

Now we are able to calculate perturbatively the form factors  $F_0^{B \rightarrow \eta^{(\prime)}}(0)$ ,  $A_{0,1}^{B \rightarrow \rho}(0)$ , and the decay amplitudes for the Feynman diagrams after the integration over  $x_i$  and  $b_i$ . When doing the above integrations over  $x_i$  and  $b_i$ , we should include the corresponding Wilson coefficients  $C_i(t_j)$  calculated at the appropriate scale  $t_j$  using Eqs. (C1) and (D1) of Ref. [9]. Since we here calculated the form factors and amplitudes at the leading order (one order of  $\alpha_s(t)$ ), the radiative corrections at the next order would emerge in terms of  $\alpha_s(t) \ln(m/t)$ , where  $m$ 's denote some scales, like  $m_B, 1/b_i, \dots$ , in the hard part  $H(t)$ . We select the largest energy scale among  $m$ 's appearing in each diagram as the hard scale  $t$ 's

for the purpose of at least killing the large logarithmic corrections partially,

$$\begin{aligned}
t_e^1 &= a_t \cdot \max(\sqrt{x_3}m_B, 1/b_1, 1/b_3) , \\
t_e^2 &= a_t \cdot \max(\sqrt{x_1}m_B, 1/b_1, 1/b_3) , \\
t_e^3 &= a_t \cdot \max(\sqrt{x_3}m_B, 1/b_2, 1/b_3) , \\
t_e^4 &= a_t \cdot \max(\sqrt{x_2}m_B, 1/b_2, 1/b_3) , \\
t_f &= a_t \cdot \max(\sqrt{x_1x_3}m_B, \sqrt{x_2x_3}m_B, 1/b_1, 1/b_2) , \\
t_f^1 &= a_t \cdot \max(\sqrt{x_2x_3}m_B, 1/b_1, 1/b_2) , \\
t_f^2 &= a_t \cdot \max(\sqrt{x_1 + x_2 + x_3 - x_1x_3 - x_2x_3}m_B, \sqrt{x_2x_3}m_B, 1/b_1, 1/b_2) , 
\end{aligned} \tag{35}$$

where the constant  $a_t = 1 \pm 0.1$  is introduced in order to estimate the scale dependence of the theoretical predictions for the observables.

Before we put the things together to write down the decay amplitudes for the studied decay modes, we give a brief discussion about the  $\eta$ - $\eta'$  mixing and the gluonic component of the  $\eta'$  meson.

The  $\eta$  and  $\eta'$  are neutral pseudoscalar ( $J^P = 0^-$ ) mesons, and usually considered as mixtures of the  $SU(3)_F$  singlet  $\eta_1$  and the octet  $\eta_8$ :

$$\begin{pmatrix} \eta \\ \eta' \end{pmatrix} = \begin{pmatrix} \cos \theta_p & -\sin \theta_p \\ \sin \theta_p & \cos \theta_p \end{pmatrix} \begin{pmatrix} \eta_8 \\ \eta_1 \end{pmatrix}, \tag{36}$$

with

$$\begin{aligned}
\eta_8 &= \frac{1}{\sqrt{6}} (u\bar{u} + d\bar{d} - 2s\bar{s}), \\
\eta_1 &= \frac{1}{\sqrt{3}} (u\bar{u} + d\bar{d} + s\bar{s}),
\end{aligned} \tag{37}$$

where  $\theta_p$  is the mixing angle to be determined by various related experiments [27]. From previous studies, one obtains the mixing angle  $\theta_p$  between  $-20^\circ$  to  $-10^\circ$ . One best fit result as given in Ref. [28] is  $-17^\circ \leq \theta_p \leq -10^\circ$ .

As shown in Eqs. (36,37),  $\eta$  and  $\eta'$  are generally considered as a linear combination of light quark pairs. But it should be noted that the  $\eta'$  meson may has a gluonic component in order to interpret the anomalously large branching ratios of  $B \rightarrow K\eta'$  and  $J/\Psi \rightarrow \eta'\gamma$  [28, 29]. In Refs. [28, 29, 30], the physical states  $\eta$  and  $\eta'$  were defined as

$$\begin{aligned}
|\eta\rangle &= X_\eta \left| \frac{u\bar{u} + d\bar{d}}{\sqrt{2}} \right\rangle + Y_\eta |s\bar{s}\rangle, \\
|\eta'\rangle &= X_{\eta'} \left| \frac{u\bar{u} + d\bar{d}}{\sqrt{2}} \right\rangle + Y_{\eta'} |s\bar{s}\rangle + Z_{\eta'} |gluonium\rangle,
\end{aligned} \tag{38}$$

where  $X_{\eta^{(\prime)}}, Y_{\eta^{(\prime)}}$  and  $Z_{\eta'}$  parameters describe the ratios of  $u\bar{u} + d\bar{d}$ ,  $s\bar{s}$  and gluonium ( $SU(3)_F$  singlet) component of  $\eta^{(\prime)}$ , respectively. In Ref.[28], the author shows that the gluonic admixture in  $\eta'$  can be as large as 26%, i.e.

$$Z_{\eta'} / (X_{\eta^{(\prime)}} + Y_{\eta^{(\prime)}} + Z_{\eta'}) \leq 0.26. \tag{39}$$

According to paper [29], a large SU(3) singlet contribution can help us to explain the large branching ratio for  $B \rightarrow K\eta'$  decay, but also result in a large branching ratio for  $B \rightarrow K^0\eta$  decay,  $Br(B \rightarrow K^0\eta) \sim 7.0(13) \times 10^{-6}$  for  $\theta_P = -20^\circ(-10^\circ)$  as given in Table II of Ref. [29], which is clearly too large than currently available upper limits [19]:

$$Br(B \rightarrow K^0\eta) < 1.9 \times 10^{-6}. \quad (40)$$

Although a lot of studies have been done along this direction, but we currently still do not understand the anomalous  $gg - \eta'$  coupling clearly, and do not know how to calculate reliably the contributions induced by the gluonic component of  $\eta'$  meson. In this paper, we firstly assume that  $\eta'$  does not have the gluonic component, and set the quark content of  $\eta$  and  $\eta'$  as described by Eqs. (36,37). We will also discuss the effects of a non-zero gluonic admixture of  $\eta'$  in next section.

Combining the contributions from different diagrams, the total decay amplitude for  $B^+ \rightarrow \rho^+\eta$  decay can be written as

$$\begin{aligned} \sqrt{3}\mathcal{M}(\rho^+\eta) = & F_{e\rho} \left\{ \left[ \xi_u \left( C_1 + \frac{1}{3}C_2 \right) - \xi_t \left( -\frac{1}{3}C_3 - C_4 - \frac{3}{2}C_7 - \frac{1}{2}C_8 + \frac{5}{3}C_9 \right. \right. \right. \\ & \left. \left. \left. + C_{10} \right) \right] f_\eta^d F_1(\theta_p) - \xi_t \left( \frac{1}{2}C_7 + \frac{1}{6}C_8 - \frac{1}{2}C_9 - \frac{1}{6}C_{10} \right) f_\eta^s F_2(\theta_p) \right\} \\ & - F_{e\rho}^P \xi_t \left( \frac{1}{3}C_5 + C_6 - \frac{1}{6}C_7 - \frac{1}{2}C_8 \right) F_1(\theta_p) \\ & + M_{e\rho} \left\{ \left[ \xi_u C_2 - \xi_t \cdot \left( C_3 + 2C_4 + 2C_6 + \frac{1}{2}C_8 - \frac{1}{2}C_9 + \frac{1}{2}C_{10} \right) \right] F_1(\theta_p) \right. \\ & \left. - \xi_t \left( C_4 + C_6 - \frac{1}{2}C_8 - \frac{1}{2}C_{10} \right) F_2(\theta_p) \right\} \\ & + (M_{a\rho} + M_e + M_a) [\xi_u C_1 - \xi_t (C_3 + C_9)] \cdot F_1(\theta_p) \\ & - (2M_{a\rho}^P + M_e^P) \xi_t (C_5 + C_7) \cdot F_1(\theta_p) \\ & + F_e \left\{ \left[ \xi_u \left( \frac{1}{3}C_1 + C_2 \right) - \xi_t \left( \frac{1}{3}C_3 + C_4 + \frac{1}{3}C_9 + C_{10} \right) \right] F_1(\theta_p) \right\}, \quad (41) \end{aligned}$$

where  $\xi_u = V_{ub}^* V_{ud}$ ,  $\xi_t = V_{tb}^* V_{td}$ , and  $F_1(\theta_p) = -\sin\theta_p + \cos\theta_p/\sqrt{2}$  and  $F_2(\theta_p) = -\sin\theta_p - \sqrt{2}\cos\theta_p$  are the mixing factors. The Wilson coefficients  $C_i$  should be calculated at the appropriate scale  $t$  using equations as given in the Appendices of Ref.[9].

Similarly, the decay amplitude for  $B^0 \rightarrow \rho^0 \eta$  can be written as

$$\begin{aligned}
\sqrt{6}\mathcal{M}(\rho^0 \eta) = & F_e \left[ \xi_u \left( C_1 + \frac{1}{3}C_2 \right) - \xi_t \left( -\frac{1}{3}C_3 - C_4 + \frac{3}{2}C_7 + \frac{1}{2}C_8 + \frac{5}{3}C_9 + C_{10} \right) \right] F_1(\theta_p) \\
& - F_{e\rho} \left\{ \left[ \xi_u \left( C_1 + \frac{1}{3}C_2 \right) \right. \right. \\
& \left. \left. - \xi_t \left( \frac{1}{3}C_3 + C_4 - \frac{1}{2}C_7 - \frac{1}{6}C_8 + \frac{1}{3}C_9 - \frac{1}{3}C_{10} \right) \right] f_\eta^d F_1(\theta_p) \right. \\
& \left. + \xi_t \left( \frac{1}{2}C_7 + \frac{1}{6}C_8 + \frac{1}{2}C_9 + \frac{1}{6}C_{10} \right) f_\eta^s F_2(\theta_p) \right\} \\
& + F_{e\rho}^P \xi_t \left( \frac{1}{3}C_5 + C_6 - \frac{1}{6}C_7 - \frac{1}{2}C_8 \right) \cdot F_1(\theta_p) \\
& - M_{e\rho} \left\{ \left[ \xi_u C_2 - \xi_t \left( C_3 + 2C_4 + 2C_6 + \frac{1}{2}C_8 - \frac{1}{2}C_9 + \frac{1}{2}C_{10} \right) \right] \cdot F_1(\theta_p) \right. \\
& \left. - \xi_t \left( C_4 + C_6 - \frac{1}{2}C_8 - \frac{1}{2}C_{10} \right) F_2(\theta_p) \right\} \\
& + (M_{a\rho} + M_a) \left[ \xi_u C_2 - \xi_t \left( -C_3 + \frac{3}{2}C_8 + \frac{1}{2}C_9 + \frac{3}{2}C_{10} \right) \right] F_1(\theta_p) \\
& - (M_e^P + 2M_a^P) \xi_t \left( C_5 - \frac{1}{2}C_7 \right) F_1(\theta_p) \\
& + M_e \left[ \xi_u C_2 - \xi_t \left( -C_3 - \frac{3}{2}C_8 + \frac{1}{2}C_9 + \frac{3}{2}C_{10} \right) \right] F_1(\theta_p). \tag{42}
\end{aligned}$$

The decay amplitudes for  $B \rightarrow \rho^+ \eta'$  and  $B \rightarrow \rho^0 \eta'$  can be obtained easily from Eqs.(41) and (42) by the following replacements

$$\begin{aligned}
f_\eta^d, f_\eta^s & \longrightarrow f_{\eta'}^d, f_{\eta'}^s, \\
F_1(\theta_p) & \longrightarrow F_1'(\theta_p) = \cos \theta_p + \frac{\sin \theta_p}{\sqrt{2}}, \\
F_2(\theta_p) & \longrightarrow F_2'(\theta_p) = \cos \theta_p - \sqrt{2} \sin \theta_p. \tag{43}
\end{aligned}$$

Note that the possible gluonic component of  $\eta'$  meson has been neglected here.

## IV. NUMERICAL RESULTS AND DISCUSSIONS

### A. Input parameters and wave functions

We use the following input parameters in the numerical calculations

$$\begin{aligned}
\Lambda_{\text{MS}}^{(f=4)} &= 250\text{MeV}, \quad f_\pi = 130\text{MeV}, \quad f_B = 190\text{MeV}, \\
m_0^{\eta_{d\bar{d}}} &= 1.4\text{GeV}, \quad f_\rho = 200\text{MeV}, \quad f_K = 160\text{MeV}, \\
M_B &= 5.2792\text{GeV}, \quad M_W = 80.41\text{GeV}. \tag{44}
\end{aligned}$$

The central values of the CKM matrix elements to be used in numerical calculations are [27]

$$\begin{aligned} |V_{ud}| &= 0.9745, & |V_{ub}| &= 0.0040, \\ |V_{tb}| &= 0.9990, & |V_{td}| &= 0.0075. \end{aligned} \quad (45)$$

For the  $B$  meson wave function, we adopt the model

$$\phi_B(x, b) = N_B x^2 (1-x)^2 \exp \left[ -\frac{M_B^2 x^2}{2\omega_b^2} - \frac{1}{2}(\omega_b b)^2 \right], \quad (46)$$

where  $\omega_b$  is a free parameter and we take  $\omega_b = 0.4 \pm 0.04$  GeV in numerical calculations, and  $N_B = 91.745$  is the normalization factor for  $\omega_b = 0.4$ . This is the same wave functions as in Refs. [9, 10, 23, 24], which is a best fit for most of the measured hadronic B decays.

For the light meson wave function, we neglect the  $b$  dependant part, which is not important in numerical analysis. We choose the wave function of  $\rho$  meson similar to the pion case [25]

$$\phi_\rho(x) = \frac{3}{\sqrt{6}} f_\rho x(1-x) \left[ 1 + 0.18 C_2^{3/2} (2x-1) \right], \quad (47)$$

$$\begin{aligned} \phi_\rho^t(x) &= \frac{f_\rho^T}{2\sqrt{6}} \left\{ 3(2x-1)^2 + 0.3(2x-1)^2 [5(2x-1)^2 - 3] \right. \\ &\quad \left. + 0.21[3 - 30(2x-1)^2 + 35(2x-1)^4] \right\}, \end{aligned} \quad (48)$$

$$\phi_\rho^s(x) = \frac{3}{2\sqrt{6}} f_\rho^T (1-2x) \left[ 1 + 0.76(10x^2 - 10x + 1) \right]. \quad (49)$$

The Gegenbauer polynomial is defined by

$$C_2^{3/2}(t) = \frac{3}{2} (5t^2 - 1). \quad (50)$$

For  $\eta$  meson's wave function,  $\phi_{\eta d\bar{d}}^A$ ,  $\phi_{\eta d\bar{d}}^P$  and  $\phi_{\eta d\bar{d}}^T$  represent the axial vector, pseudoscalar and tensor components of the wave function respectively, for which we utilize the result from the light-cone sum rule [31] including twist-3 contribution:

$$\begin{aligned} \phi_{\eta d\bar{d}}^A(x) &= \frac{3}{\sqrt{2N_c}} f_x x(1-x) \left\{ 1 + a_2^{\eta d\bar{d}} \frac{3}{2} [5(1-2x)^2 - 1] \right. \\ &\quad \left. + a_4^{\eta d\bar{d}} \frac{15}{8} [21(1-2x)^4 - 14(1-2x)^2 + 1] \right\}, \\ \phi_{\eta d\bar{d}}^P(x) &= \frac{1}{2\sqrt{2N_c}} f_x \left\{ 1 + \frac{1}{2} \left( 30\eta_3 - \frac{5}{2}\rho_{\eta d\bar{d}}^2 \right) [3(1-2x)^2 - 1] \right. \\ &\quad \left. + \frac{1}{8} \left( -3\eta_3\omega_3 - \frac{27}{20}\rho_{\eta d\bar{d}}^2 - \frac{81}{10}\rho_{\eta d\bar{d}}^2 a_2^{\eta d\bar{d}} \right) [35(1-2x)^4 - 30(1-2x)^2 + 3] \right\}, \\ \phi_{\eta d\bar{d}}^T(x) &= \frac{3}{\sqrt{2N_c}} f_x (1-2x) \\ &\quad \cdot \left[ \frac{1}{6} + (5\eta_3 - \frac{1}{2}\eta_3\omega_3 - \frac{7}{20}\rho_{\eta d\bar{d}}^2 - \frac{3}{5}\rho_{\eta d\bar{d}}^2 a_2^{\eta d\bar{d}})(10x^2 - 10x + 1) \right], \end{aligned} \quad (51)$$

with

$$\begin{aligned} a_2^{\eta_{d\bar{d}}} &= 0.44, & a_4^{\eta_{d\bar{d}}} &= 0.25, & a_1^K &= 0.20, & a_2^K &= 0.25, \\ \rho_{\eta_{d\bar{d}}} &= m_\pi/m_0^{\eta_{d\bar{d}}}, & \eta_3 &= 0.015, & \omega_3 &= -3.0. \end{aligned} \quad (52)$$

We assume that the wave function of  $u\bar{u}$  is same as the wave function of  $d\bar{d}$ . For the wave function of the  $s\bar{s}$  components, we also use the same form as  $d\bar{d}$  but with  $m_0^{s\bar{s}}$  and  $f_y$  instead of  $m_0^{d\bar{d}}$  and  $f_x$ , respectively. For  $f_x$  and  $f_y$ , we use the values as given in Ref. [32] where isospin symmetry is assumed for  $f_x$  and  $SU(3)$  breaking effect is included for  $f_y$ :

$$f_x = f_\pi, \quad f_y = \sqrt{2f_K^2 - f_\pi^2}. \quad (53)$$

These values are translated to the values in the two mixing angle method, which is often used in vacuum saturation approach as:

$$\begin{aligned} f_8 &= 169\text{MeV}, & f_1 &= 151\text{MeV}, \\ \theta_8 &= -25.9^\circ(-18.9^\circ), & \theta_1 &= -7.1^\circ(-0.1^\circ), \end{aligned} \quad (54)$$

where the pseudoscalar mixing angle  $\theta_p$  is taken as  $-17^\circ$  ( $-10^\circ$ ) [28]. The parameters  $m_0^i$  ( $i = \eta_{d\bar{d}(u\bar{u})}, \eta_{s\bar{s}}$ ) are defined as:

$$m_0^{\eta_{d\bar{d}(u\bar{u})}} \equiv m_0^\pi \equiv \frac{m_\pi^2}{(m_u + m_d)}, \quad m_0^{\eta_{s\bar{s}}} \equiv \frac{2M_K^2 - m_\pi^2}{(2m_s)}. \quad (55)$$

We include full expression of twist-3 wave functions for light mesons. The twist-3 wave functions are also adopted from QCD sum rule calculations [33]. We will see later that this set of parameters will give good results for  $B \rightarrow \rho\eta^{(\prime)}$  decays. Using the above chosen wave functions and the central values of relevant input parameters, we find the numerical values of the corresponding form factors at zero momentum transfer from Eqs.(20) and (28)

$$\begin{aligned} A_0^{B \rightarrow \rho}(q^2 = 0) &= 0.37, \\ F_0^{B \rightarrow \eta}(q^2 = 0) &= 0.15, \\ F_0^{B \rightarrow \eta'}(q^2 = 0) &= 0.14. \end{aligned} \quad (56)$$

These values agree well with those as given in Refs. [31, 32, 34].

## B. Branching ratios

For  $B \rightarrow \rho\eta^{(\prime)}$  decays, the decay amplitudes in Eqs. (41) and (42) can be rewritten as

$$\mathcal{M} = V_{ub}^* V_{ud} T - V_{tb}^* V_{td} P = V_{ub}^* V_{ud} T [1 + z e^{i(\alpha+\delta)}], \quad (57)$$

where

$$z = \left| \frac{V_{tb}^* V_{td}}{V_{ub}^* V_{ud}} \right| \left| \frac{P}{T} \right| \quad (58)$$

is the ratio of penguin to tree contributions,  $\alpha = \arg \left[ -\frac{V_{td}V_{tb}^*}{V_{ud}V_{ub}^*} \right]$  is the weak phase (one of the three CKM angles), and  $\delta$  is the relative strong phase between tree (T) and penguin (P) diagrams. The ratio  $z$  and the strong phase  $\delta$  can be calculated in our PQCD approach. One can leave the CKM angle  $\alpha$  as a free parameter and explore the CP asymmetry parameter dependence on it.

For  $B \rightarrow \rho^+\eta$  decay, for example, one can find “T” and “P” terms by comparing the decay amplitude as defined in Eq. (41) with that in Eq. (57),

$$T(\rho^+\eta) = \frac{F_1(\theta_p)}{\sqrt{3}} \cdot \left\{ F_{e\rho} \left( C_1 + \frac{1}{3}C_2 \right) f_\eta^d + M_{e\rho}C_2 \right. \\ \left. + F_e \left( \frac{1}{3}C_1 + C_2 \right) + (M_a + M_e + M_{a\rho}) C_1 \right\}, \quad (59)$$

$$P(\rho^+\eta) = \frac{F_1(\theta_p)}{\sqrt{3}} \cdot \left\{ F_{e\rho} \left( -\frac{1}{3}C_3 - C_4 - \frac{3}{2}C_7 - \frac{1}{2}C_8 + \frac{5}{3}C_9 + C_{10} \right) f_\eta^d \right. \\ \left. + F_{e\rho}^P \left( \frac{1}{3}C_5 + C_6 - \frac{1}{6}C_7 - \frac{1}{2}C_8 \right) \right. \\ \left. + M_{e\rho} \left( -C_3 + 2C_6 - \frac{3}{2}C_8 + \frac{1}{2}C_9 + \frac{3}{2}C_{10} \right) \right. \\ \left. + F_e \left( \frac{1}{3}C_3 + C_4 + \frac{1}{3}C_9 + C_{10} \right) \right. \\ \left. + (M_{a\rho} + M_e + M_a) (C_3 + C_9) + (2M_a^P + M_e^P) (C_5 + C_7) \right\} \\ + \frac{F_2(\theta_p)}{\sqrt{3}} \left\{ F_{e\rho} \left( \frac{1}{2}C_7 + \frac{1}{6}C_8 - \frac{1}{2}C_9 - \frac{1}{6}C_{10} \right) \cdot f_\eta^s \right. \\ \left. + M_{e\rho} \left( C_4 + C_6 - \frac{1}{2}C_8 - \frac{1}{2}C_{10} \right) \right\}. \quad (60)$$

Similarly, one can obtain the expressions of the corresponding tree and penguin terms for the remaining three decays.

Using the “T” and “P” terms, one can calculate the ratio  $z$  and the strong phase  $\delta$  for the decay in study. For  $B^+ \rightarrow \rho^+\eta$  and  $\rho^+\eta'$  decays, we find numerically that

$$z(\rho^+\eta) = 0.10, \quad \delta(\rho^+\eta) = -137^\circ, \quad (61)$$

$$z(\rho^+\eta') = 0.15, \quad \delta(\rho^+\eta') = -139^\circ. \quad (62)$$

The errors of the ratio  $z$  and the strong phase  $\delta$  induced by the uncertainty of the input parameters, such as  $\omega_b = 0.4 \pm 0.04$  GeV,  $m_0^\pi = 1.4 \pm 0.1$  GeV, and  $\alpha = 100^\circ \pm 20^\circ$ , are very small in magnitude and not be shown explicitly in Eqs. (61) and (62). The reason is that the errors induced by the uncertainties of these input parameters are canceled almost completely in the ratio.

Unlike the case of QCD factorization approach, the energy scale  $t$  (in PQCD factorization approach) appeared in the Wilson coefficients  $C_i(t)$  and in the Sudakov form factors  $S_j(t)$  vary simultaneously during the integration over  $x_i$  and  $b_i$  ( $i = 1, 2, 3$ ). If we choose the hard energy scale  $t_j'$ s as defined in Eqs. (35) with  $a_t = 1$ , there will be no remaining scale dependence left explicitly after the integration. But we know that such

scale dependence should exist and likely dominate the errors on theoretical predictions for those observables. Since the calculation in this paper is performed at the leading order and thus may suffer from the uncertainties due to the scale dependence of the LO Wilson coefficients. In Ref. [37] the authors calculated the branching ratios of  $B \rightarrow K\pi, \pi\pi$  firstly at the next-to-leading order by using the PQCD factorization approach, and they found that the NLO contribution can give about 15 – 20% correction to LO predictions. The size of NLO contribution in PQCD approach is indeed very complicated to calculate. To explore it, as shown in Eq. (35), we here multiply a factor  $a_t = 1 \pm 0.1$  to the ordinary definition of scale  $t_j$ 's in Refs. [9, 10, 11, 12, 13], and take it as an estimation for the uncertainty of the possible scale dependence. Numerically we find that

$$z(\rho^+\eta) = 0.10_{-0.01}^{+0.06}, \quad \delta(\rho^+\eta) = (-137_{-2}^{+22})^\circ, \quad (63)$$

$$z(\rho^+\eta') = 0.15_{-0.01}^{+0.06}, \quad \delta(\rho^+\eta') = (-139_{-1}^{+27})^\circ, \quad (64)$$

for  $a_t = 1 \pm 0.1$ . The larger change of  $z$  and  $\delta$  corresponds to the case of  $a_t = 0.9$ , while the magnitude of the variations is consistent with the general expectation.

From Eq. (57), it is easy to write the decay amplitude for the corresponding charge conjugated decay mode

$$\overline{\mathcal{M}} = V_{ub}V_{ud}^*T - V_{tb}V_{td}^*P = V_{ub}V_{ud}^*T [1 + ze^{i(-\alpha+\delta)}]. \quad (65)$$

Therefore the CP-averaged branching ratio for  $B^0 \rightarrow \rho\eta^{(\prime)}$  is

$$Br = (|\mathcal{M}|^2 + |\overline{\mathcal{M}}|^2)/2 = |V_{ub}V_{ud}^*T|^2 [1 + 2z \cos \alpha \cos \delta + z^2], \quad (66)$$

where the ratio  $z$  and the strong phase  $\delta$  have been defined in Eqs.(57) and (58). It is easy to see that the CP-averaged branching ratio is a function of  $\cos \alpha$  for the given ratio  $z$  and the strong phase  $\delta$ . This gives a potential method to determine the CKM angle  $\alpha$  by measuring only the CP-averaged branching ratios with PQCD calculations. But one should know that the uncertainty of theory is so large as to make it unrealistic.

Using the wave functions and the input parameters as specified in previous sections, it is straightforward to calculate the branching ratios for the four considered decays. The theoretical predictions in the PQCD approach for the branching ratios of the decays under consideration are the following

$$Br(B^+ \rightarrow \rho^+\eta) = [8.5_{-2.1}^{+3.0}(\omega_b)_{-0.7}^{+0.8}(m_0^\pi) \pm 0.4(\alpha)_{-0.2}^{+1.2}(a_t)] \times 10^{-6}, \quad (67)$$

$$Br(B^+ \rightarrow \rho^+\eta') = [8.7_{-2.2}^{+3.0}(\omega_b)_{-0.9}^{+0.7}(m_0^\pi)_{-0.7}^{+0.5}(\alpha)_{-0.3}^{+1.1}(a_t)] \times 10^{-6}, \quad (68)$$

$$Br(B^0 \rightarrow \rho^0\eta) = [0.024_{-0.007}^{+0.012}(\omega_b)_{-0.002}^{+0.004}(m_0^\pi) \pm 0.002(\alpha)_{-0.005}^{+0.102}(a_t)] \times 10^{-6}, \quad (69)$$

$$Br(B^0 \rightarrow \rho^0\eta') = [0.061_{-0.018}^{+0.030}(\omega_b)_{-0.003}^{+0.004}(m_0^\pi) \pm 0.003(\alpha)_{-0.009}^{+0.114}(a_t)] \times 10^{-6}, \quad (70)$$

for  $\theta_p = -10^\circ$ ; and

$$Br(B^+ \rightarrow \rho^+\eta) = [10.6_{-2.6}^{+3.9}(\omega_b)_{-0.9}^{+1.0}(m_0^\pi) \pm 0.5(\alpha)_{-0.3}^{+1.4}(a_t)] \times 10^{-6}, \quad (71)$$

$$Br(B^+ \rightarrow \rho^+\eta') = [6.5_{-1.8}^{+2.3}(\omega_b) \pm 0.6(m_0^\pi) \pm 0.5(\alpha)_{-0.2}^{+0.9}(a_t)] \times 10^{-6}, \quad (72)$$

$$Br(B^0 \rightarrow \rho^0\eta) = [0.042_{-0.012}^{+0.020}(\omega_b) \pm 0.005(m_0^\pi)_{-0.004}^{+0.006}(\alpha)_{-0.012}^{+0.128}(a_t)] \times 10^{-6}, \quad (73)$$

$$Br(B^0 \rightarrow \rho^0\eta') = [0.047_{-0.016}^{+0.020}(\omega_b)_{-0.006}^{+0.001}(m_0^\pi) \pm 0.001(\alpha)_{-0.004}^{+0.100}(a_t)] \times 10^{-6}, \quad (74)$$

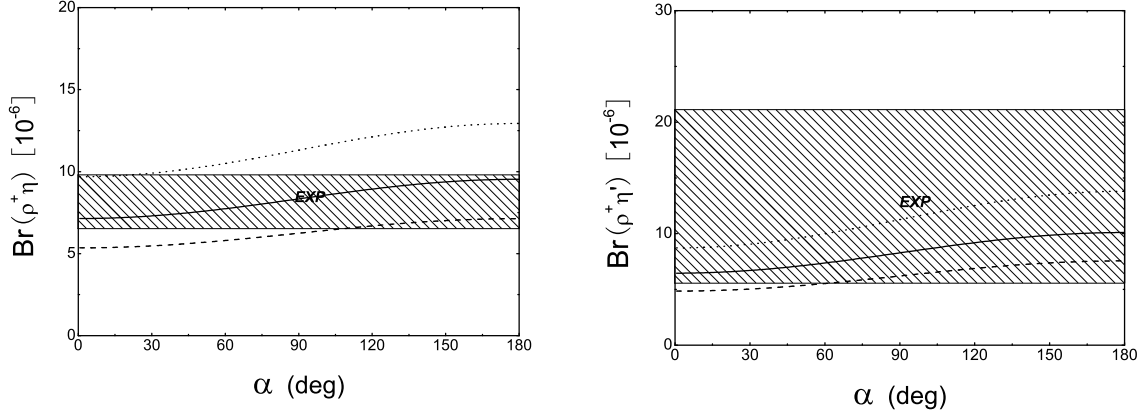


FIG. 3: The  $\alpha$  dependence of the branching ratios (in unit of  $10^{-6}$ ) of  $B^+ \rightarrow \rho^+ \eta^{(\prime)}$  decay for  $m_0^\pi = 1.4$  GeV,  $\theta_p = -10^\circ$ ,  $\omega_b = 0.36$  GeV (dotted curve),  $0.40$  GeV (solid curve) and  $0.44$  GeV (short-dashed curve). The gray band show the data.

for  $\theta_p = -17^\circ$ . The major errors are induced by the uncertainty of hard energy scale  $t$ ,  $\omega_b = 0.4 \pm 0.04$  GeV,  $m_0^\pi = 1.4 \pm 0.1$  GeV and  $\alpha = 100^\circ \pm 20^\circ$ , respectively. It is easy to see that (a) the errors of the branching ratios induced by varying  $a_t$  in the range of  $a_t = [0.9, 1.1]$  are less than 20% for the tree-dominated  $B \rightarrow \rho^+ \eta^{(\prime)}$  decays; but can be significant for the penguin-dominated  $B \rightarrow \rho^0 \eta^{(\prime)}$  decays; and (b) the variations with respect to the central values are large (small) for the case of  $a_t = 0.9$  ( $a_t = 1.1$ ). This feature agrees with general expectations: when the scale  $t$  become smaller, the reliability of the perturbative calculation of the form factors in PQCD approach will become weak!

It is easy to see that the PQCD predictions for the branching ratios of considered decays agree very well with the measured values or the upper limits as shown in Eqs.(1) and (2). For the four  $B \rightarrow \rho \eta^{(\prime)}$  decays, the theoretical predictions for the CP-averaged branching ratios in the PQCD approach are well consistent with those given in the QCD factorization approach [2]:

$$\begin{aligned} Br(B^+ \rightarrow \rho^+ \eta) &= (9.4_{-4.8}^{+5.9}) \times 10^{-6}, \\ Br(B^+ \rightarrow \rho^+ \eta') &= (6.3_{-3.3}^{+4.0}) \times 10^{-6}, \end{aligned} \quad (75)$$

$$\begin{aligned} Br(B^0 \rightarrow \rho^0 \eta) &= (0.03_{-0.10}^{+0.17}) \times 10^{-6}, \\ Br(B^0 \rightarrow \rho^0 \eta') &= (0.01_{-0.06}^{+0.12}) \times 10^{-6}, \end{aligned} \quad (76)$$

where the individual errors have been added in quadrature.

It is worth stressing that the theoretical predictions in the PQCD approach have large theoretical errors induced by our ignorance of NLO contributions, and the still large uncertainties of many input parameters. In our analysis, we consider the constraints on these parameters from analysis of other well measured decay channels. For example, the constraint  $1.1\text{GeV} \leq m_0^\pi \leq 1.9\text{GeV}$  was obtained from the phenomenological studies for  $B \rightarrow \pi\pi$  decays [9], while the constraint of  $\alpha \approx 100^\circ \pm 20^\circ$  were obtained by direct measurements or from the global fit [19, 35, 36]. From numerical calculations, we get to

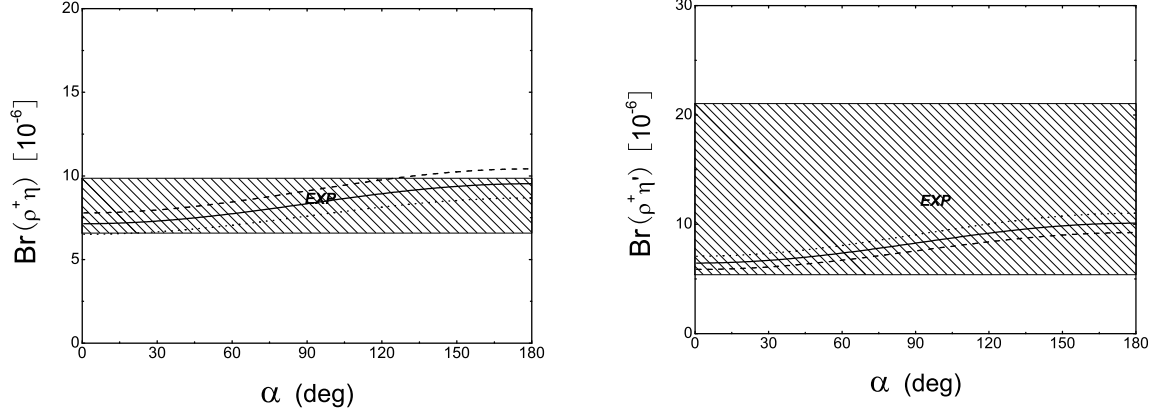


FIG. 4: The  $\alpha$  dependence of the branching ratios (in unit of  $10^{-6}$ ) of  $B^+ \rightarrow \rho^+ \eta^{(\prime)}$  decays for  $\omega_b = 0.4$  GeV,  $\theta_p = -10^\circ$ ,  $m_0^\pi = 1.3$  GeV (dotted curve), 1.4 GeV (solid curve) and 1.5 GeV (short-dashed curve). The gray band shows the data.

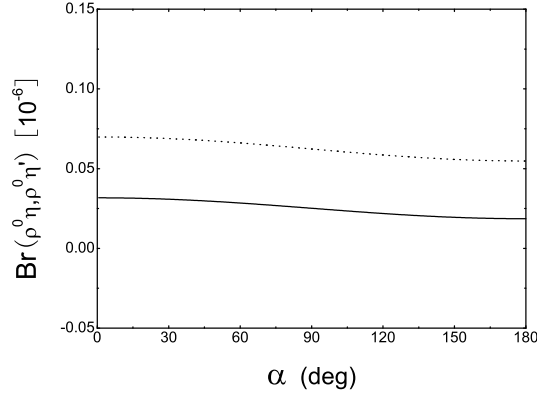


FIG. 5: The  $\alpha$  dependence of the branching ratios (in unit of  $10^{-6}$ ) of  $\rho^0 \eta$  (solid curve) and  $\rho^0 \eta'$  (dotted curve) decays for  $m_0^\pi = 1.4$  GeV,  $\theta_p = -10^\circ$ ,  $\omega_b = 0.40$  GeV.

know that the main errors come from the uncertainty of  $\omega_b$ ,  $m_0^\pi$ ,  $\alpha$ ,  $\theta_p$  and the next-to-leading order contributions.

In Figs. 3 and 4, we present, respectively, the PQCD predictions of the branching ratios of  $B \rightarrow \rho^+ \eta$  and  $\rho^+ \eta'$  decays for  $\theta_p = 10^\circ$ ,  $\omega_b = 0.4 \pm 0.04$  GeV,  $m_0^\pi = 1.4 \pm 0.1$  GeV and  $\alpha = [0^\circ, 180^\circ]$ . Fig. 5 shows the  $\alpha$ -dependence of the PQCD predictions of the branching ratios of  $B \rightarrow \rho^0 \eta^{(\prime)}$  decays for  $\theta_p = 10^\circ$ ,  $\omega_b = 0.4$  GeV,  $m_0^\pi = 1.4$  GeV and  $\alpha = [0^\circ, 180^\circ]$ .

From the numerical results and the figures we observe that the PQCD predictions are very sensitive to the variations of  $\omega_b$  and  $m_0^\pi$ . The parameter  $m_0^\pi$  originates from the chiral perturbation theory and have a value near 1 GeV. The  $m_0^\pi$  parameter characterizes the relative size of twist 3 contribution to twist 2 contribution. Because of the chiral

enhancement of  $m_0^\pi$ , the twist 3 contribution become comparable in size with the twist 2 contribution. The branching ratios of  $Br(B \rightarrow \rho\eta^{(\prime)})$  are also sensitive to the parameter  $m_0^\pi$ , but not as strong as the  $\omega_b$  dependence.

### C. CP-violating asymmetries

Now we turn to the evaluations of the CP-violating asymmetries of  $B \rightarrow \rho\eta^{(\prime)}$  decays in PQCD approach. For  $B^+ \rightarrow \rho^+\eta$  and  $B^+ \rightarrow \rho^+\eta'$  decays, the direct CP-violating asymmetries  $A_{CP}$  can be defined as:

$$\mathcal{A}_{CP}^{dir} = \frac{|\overline{\mathcal{M}}|^2 - |\mathcal{M}|^2}{|\overline{\mathcal{M}}|^2 + |\mathcal{M}|^2} = \frac{2z \sin \alpha \sin \delta}{1 + 2z \cos \alpha \cos \delta + z^2}, \quad (77)$$

where the ratio  $z$  and the strong phase  $\delta$  have been defined in previous subsection and are calculable in PQCD approach.

Using the central values of  $z$  and  $\delta$  as given in Eqs.(61) and (62), it is easy to calculate the CP-violating asymmetries. In Fig. 6, we show the  $\alpha$ -dependence of the direct CP-violating asymmetries  $\mathcal{A}_{CP}^{dir}$  for  $B^\pm \rightarrow \rho^\pm\eta$  (the solid curve) and  $B^\pm \rightarrow \rho^\pm\eta'$  (the dotted curve) decay, respectively. From Fig. 6, one can see that the CP-violating asymmetries  $A_{CP}^{dir}(B^\pm \rightarrow \rho^\pm\eta)$  and  $A_{CP}^{dir}(B^\pm \rightarrow \rho^\pm\eta')$  are large in magnitude, about  $-15\%$  for  $\alpha \sim 100^\circ$ . The large CP-violating asymmetries plus large branching ratios are clearly measurable in the B factory experiments.

For  $\alpha = 100^\circ \pm 20^\circ$ , one can read out the allowed ranges of  $A_{CP}^{dir}$  from Fig. 6 directly

$$\begin{aligned} A_{CP}^{dir}(B^\pm \rightarrow \rho^\pm\eta) &= (-13_{-0.5}^{+1.2}(\alpha)_{-14}^{+2}(a_t)) \times 10^{-2}, \\ A_{CP}^{dir}(B^\pm \rightarrow \rho^\pm\eta') &= (-18_{-1.6}^{+3.0}(\alpha)_{-14}^{+1}(a_t)) \times 10^{-2}. \end{aligned} \quad (78)$$

where the second error comes from  $a_t = 1.0 \pm 0.1$ , it is indeed not very large. The possible theoretical errors induced by the uncertainties of other input parameters are all very small, since both  $z$  and  $\delta$  are stable against the variations of them.

The theoretical predictions for the direct CP-violating asymmetries  $A_{CP}^{dir}(B^\pm \rightarrow \rho^\pm\eta^{(\prime)})$  in the PQCD approach are generally larger in size than those obtained by using the QCD factorization approach [2]

$$\begin{aligned} A_{CP}^{dir}(B^\pm \rightarrow \rho^\pm\eta) &= (-2.4 \pm 6.4) \times 10^{-2}, \\ A_{CP}^{dir}(B^\pm \rightarrow \rho^\pm\eta') &= (4.1_{-9.9}^{+10.6}) \times 10^{-2}. \end{aligned} \quad (79)$$

On the experimental side, the new world-average [19] is

$$A_{CP}(B^\pm \rightarrow \rho^\pm\eta)^{exp} = (-3 \pm 16) \times 10^{-2}, \quad (80)$$

which is still consistent with the predictions in both PQCD and QCD factorization approach within the still large experimental error. More data are clearly needed to make a reliable judgement.

We now study the CP-violating asymmetries for  $B^0 \rightarrow \rho^0\eta^{(\prime)}$  decays. For these neutral decay modes, the effects of  $B^0 - \bar{B}^0$  mixing should be considered. For  $B^0$  meson decays,

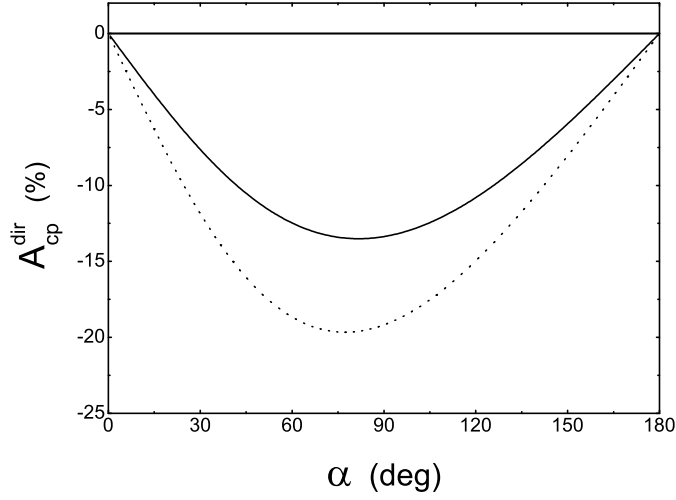


FIG. 6: The direct CP asymmetries (in percentage) of  $B^+ \rightarrow \rho^+ \eta$  (solid curve) and  $B^+ \rightarrow \rho^+ \eta'$  (dotted curve) as a function of CKM angle  $\alpha$ .

we know that  $\Delta\Gamma/\Delta m_d \ll 1$  and  $\Delta\Gamma/\Gamma \ll 1$ . The CP-violating asymmetry of  $B^0(\bar{B}^0) \rightarrow \rho^0 \eta^{(\prime)}$  decay is time dependent and can be defined as

$$\begin{aligned} A_{CP} &\equiv \frac{\Gamma(\bar{B}_d^0(\Delta t) \rightarrow f_{CP}) - \Gamma(B_d^0(\Delta t) \rightarrow f_{CP})}{\Gamma(\bar{B}_d^0(\Delta t) \rightarrow f_{CP}) + \Gamma(B_d^0(\Delta t) \rightarrow f_{CP})} \\ &= A_{CP}^{dir} \cos(\Delta m \Delta t) + A_{CP}^{mix} \sin(\Delta m \Delta t), \end{aligned} \quad (81)$$

where  $\Delta m$  is the mass difference between the two  $B^0$  mass eigenstates,  $\Delta t = t_{CP} - t_{tag}$  is the time difference between the tagged  $B^0$  ( $\bar{B}^0$ ) and the accompanying  $\bar{B}^0$  ( $B^0$ ) with opposite b flavor decaying to the final CP-eigenstate  $f_{CP}$  at the time  $t_{CP}$ . The direct and mixing induced CP-violating asymmetries  $A_{CP}^{dir}$  and  $A_{CP}^{mix}$  can be written as

$$A_{CP}^{dir} = \frac{|\lambda_{CP}|^2 - 1}{1 + |\lambda_{CP}|^2}, \quad A_{CP}^{mix} = \frac{2\text{Im}(\lambda_{CP})}{1 + |\lambda_{CP}|^2}, \quad (82)$$

where the CP-violating parameter  $\lambda_{CP}$  is

$$\lambda_{CP} = \frac{V_{tb}^* V_{td} \langle \rho^0 \eta^{(\prime)} | H_{eff} | \bar{B}^0 \rangle}{V_{tb} V_{td}^* \langle \rho^0 \eta^{(\prime)} | H_{eff} | B^0 \rangle} = e^{2i\alpha} \frac{1 + ze^{i(\delta-\alpha)}}{1 + ze^{i(\delta+\alpha)}}. \quad (83)$$

Here the ratio  $z$  and the strong phase  $\delta$  have been defined previously. In PQCD approach, since both  $z$  and  $\delta$  are calculable, it is easy to find the numerical values of  $A_{CP}^{dir}$  and  $A_{CP}^{mix}$  for the considered decay processes.

For  $B^0 \rightarrow \rho^0 \eta$  and  $\rho^0 \eta'$  decays, the numerical values of the ratio  $z$  and the strong phase  $\delta$  are

$$z(\rho^0 \eta) = 4.0, \quad \delta(\rho^0 \eta) = -57^\circ, \quad (84)$$

$$z(\rho^0 \eta') = 6.8, \quad \delta(\rho^0 \eta') = -65^\circ. \quad (85)$$

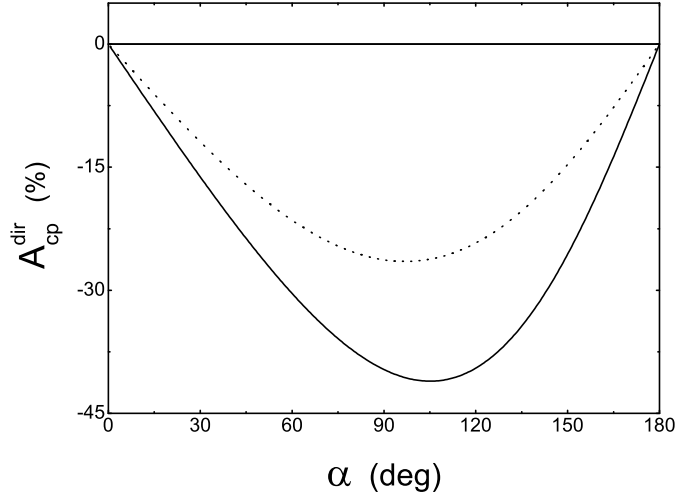


FIG. 7: The direct CP asymmetry  $A_{CP}^{dir}$  (in percentage) of  $B^0 \rightarrow \rho^0 \eta$  (solid curve) and  $B^0 \rightarrow \rho^0 \eta'$  (dotted curve) as a function of CKM angle  $\alpha$ .

Unlike the case of  $B^\pm \rightarrow \rho^\pm \eta^{(\prime)}$  decays, we here have  $z > 1$ , which means that the “P” term is much larger in size than the “T” term for  $B^0 \rightarrow \rho^0 \eta^{(\prime)}$  decays, since the “T” term here is a color-suppressed tree.

In Figs. 7 and 8, we show the  $\alpha$ -dependence of the direct and the mixing-induced CP-violating asymmetry  $A_{CP}^{dir}$  and  $A_{CP}^{mix}$  for  $B^0 \rightarrow \rho^0 \eta$  (solid curve) and  $B^0 \rightarrow \rho^0 \eta'$  (dotted curve) decays, respectively. For  $\alpha \sim 100^\circ$ , one can find numerically that

$$A_{CP}^{dir}(B^0 \rightarrow \rho^0 \eta) \approx -41\%, \quad A_{CP}^{mix}(B^0 \rightarrow \rho^0 \eta) \approx +25\%, \quad (86)$$

$$A_{CP}^{dir}(B^0 \rightarrow \rho^0 \eta') \approx -27\%, \quad A_{CP}^{mix}(B^0 \rightarrow \rho^0 \eta') \approx +11\%. \quad (87)$$

They are also large in size. The theoretical errors induced by the uncertainties of input parameters are only about 10% because of the cancelation in ratios. If we vary  $a_t$  in the range of  $0.9 \leq a_t \leq 1.1$ , however, the theoretical predictions for the CP-violating asymmetries of the penguin-dominated  $B^0 \rightarrow \rho^0 \eta^{(\prime)}$  decays may change significantly

$$A_{CP}^{dir}(B^0 \rightarrow \rho^0 \eta) = [-85\%, +24\%], \quad A_{CP}^{mix}(B^0 \rightarrow \rho^0 \eta) = [-19\%, +35\%], \quad (88)$$

$$A_{CP}^{dir}(B^0 \rightarrow \rho^0 \eta') = [-75\%, +13\%], \quad A_{CP}^{mix}(B^0 \rightarrow \rho^0 \eta') = [-9\%, +22\%]. \quad (89)$$

This feature may be interpreted as an indication of the importance of the NLO contributions to those penguin dominated decay modes.

If we integrate the time variable  $t$ , we will get the total CP asymmetry for  $B^0 \rightarrow \rho^0 \eta^{(\prime)}$  decays,

$$A_{CP} = \frac{1}{1+x^2} A_{CP}^{dir} + \frac{x}{1+x^2} A_{CP}^{mix}, \quad (90)$$

where  $x = \Delta m/\Gamma = 0.771$  for the  $B^0 - \bar{B}^0$  mixing [27]. In Fig.9, we show the  $\alpha$ -dependence of the total CP asymmetry  $A_{CP}$  for  $B^0 \rightarrow \rho^0 \eta$  (solid curve) and  $B^0 \rightarrow \rho^0 \eta'$  (dotted curve) decay, respectively. For  $\alpha \sim 100^\circ$ , the total CP asymmetry is around  $-10\%$  for  $B^0 \rightarrow \rho^0 \eta^{(\prime)}$  decays.

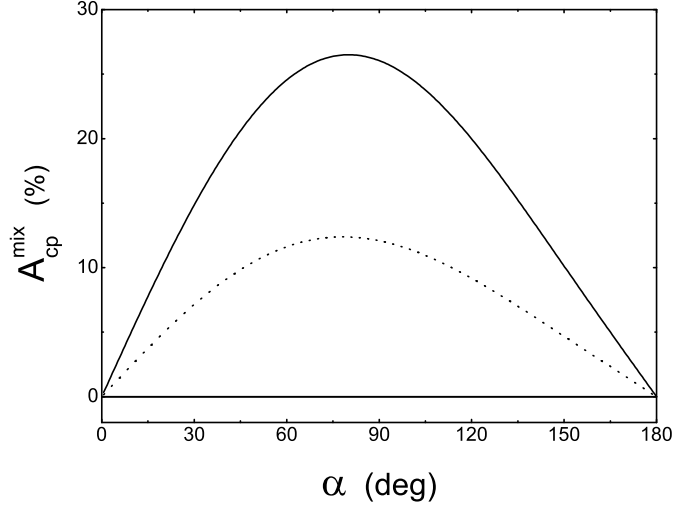


FIG. 8: The mixing induced CP asymmetry  $A_{CP}^{mix}$  (in percentage) of  $B^0 \rightarrow \rho^0 \eta$  (solid curve) and  $B^0 \rightarrow \rho^0 \eta'$  (dotted curve) as a function of CKM angle  $\alpha$ .

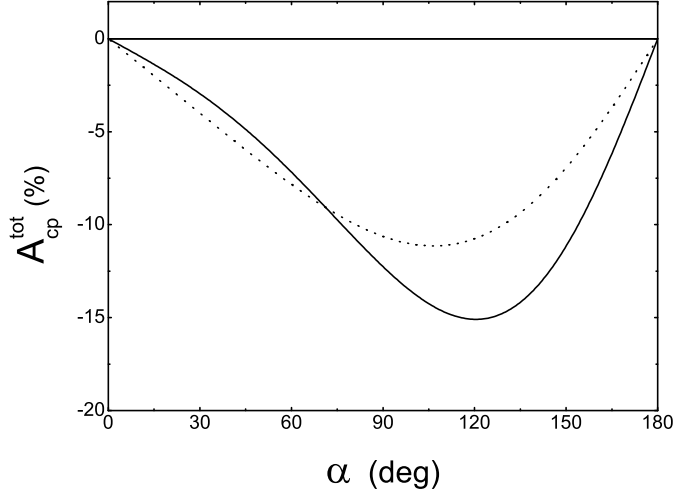


FIG. 9: The total CP asymmetry  $A_{CP}^{tot}$  (in percentage) of  $B^0 \rightarrow \rho^0 \eta$  (solid curve) and  $B^0 \rightarrow \rho^0 \eta'$  (dotted curve) as a function of CKM angle  $\alpha$ .

For  $B^+ \rightarrow \rho^+ \eta$  and  $\rho^+ \eta'$  decays, the large CP-violating asymmetry around  $-15\%$  could be measured in the running B factory experiments since their branching ratios are rather large,  $\sim 10^{-5}$ . For  $Br(B^0 \rightarrow \rho^0 \eta)$  and  $\rho^0 \eta'$  decays, however, it is very difficult to measure their CP-violating asymmetries at current running B factories since their branching ratios are very small,  $\sim 10^{-8}$  only. It could be measured in the forthcoming LHCb experiment.

#### D. Effects of possible gluonic component of $\eta'$

Up to now, we have not considered the possible contributions to the branching ratios and CP-violating asymmetries of  $B \rightarrow \rho \eta'$  decays induced by the possible gluonic component of  $\eta'$  [28, 29, 30]. When  $Z_{\eta'} \neq 0$ , a decay amplitude  $\mathcal{M}'$  will be produced by the

gluonic component of  $\eta'$ . Such decay amplitude may interfere constructively or destructively with the ones from the  $q\bar{q}$  ( $q = u, d, s$ ) components of  $\eta'$ , the branching ratios of the decays in question may be increased or decreased accordingly.

Unfortunately, we currently do not know how to calculate this kind of contributions reliably. But we can treat it as an theoretical uncertainty. For  $|M'/M(q\bar{q})| \sim 0.1 - 0.2$ , for example, the resulted uncertainty for the branching ratios as given in Eqs.(68) and (70) will be around twenty to thirty percent.

From Eq. (68), one can see that the theoretical prediction of  $Br(B^+ \rightarrow \rho^+\eta')$  in the PQCD approach agrees well with the measured value within one standard deviation, which means that there is no large room left for the contribution due to the gluonic component of  $\eta'$ . We therefore believe that the gluonic admixture of  $\eta'$  should be small, and most possibly not as important as expected before.

As for the CP-violating asymmetries of  $B \rightarrow \rho\eta'$  decays, the possible contributions of the gluonic components of the  $\eta'$  meson are largely cancelled in the ratio.

## V. SUMMARY

In this paper, we calculate the branching ratios and CP-violating asymmetries of  $B^0 \rightarrow \rho^0\eta$ ,  $B^0 \rightarrow \rho^0\eta'$ ,  $B^+ \rightarrow \rho^+\eta$ , and  $B^+ \rightarrow \rho^+\eta'$  decays in the PQCD factorization approach.

Besides the usual factorizable diagrams, the non-factorizable and annihilation diagrams as shown in Figs. (1) and (2) are also calculated analytically. Although the non-factorizable and annihilation contributions are sub-leading for the branching ratios of the considered decays, but they are not negligible. Furthermore these diagrams provide the necessary strong phase required by a non-zero CP-violating asymmetry for the considered decays.

From our calculations and phenomenological analysis, we found the following results:

- From analytical calculations, the form factors for  $B \rightarrow \eta$ ,  $B \rightarrow \eta'$  and  $B \rightarrow \rho$  transitions can be extracted. The PQCD results for these form factors are  $A_0^{B \rightarrow \rho}(0) = 0.37$ ,  $F_0^{B \rightarrow \eta}(0) = 0.15$  and  $F_0^{B \rightarrow \eta'}(0) = 0.14$ , which are in good agreement with those obtained from the QCD sum rule calculations.
- For the branching ratios of the four considered decay modes, the theoretical predictions in PQCD approach are

$$Br(B^+ \rightarrow \rho^+\eta^{(\prime)}) \approx 9 \times 10^{-6}, \quad (91)$$

$$Br(B^0 \rightarrow \rho^0\eta^{(\prime)}) \approx 5 \times 10^{-8}. \quad (92)$$

Although the theoretical uncertainties are still large (can reach 50%), the leading PQCD predictions for the branching ratios agree well with the measured values or currently available experimental upper limits, and are also consistent with the results obtained by employing the QCD factorization approach.

- For the CP-violating asymmetries, the theoretical predictions in PQCD approach

are

$$A_{CP}^{dir}(B^\pm \rightarrow \rho^\pm \eta) \approx -13\%, \quad (93)$$

$$A_{CP}^{dir}(B^\pm \rightarrow \rho^\pm \eta') \approx -18\%, \quad (94)$$

$$A_{CP}^{dir}(B^0 \rightarrow \rho^0 \eta) \approx -41\%, \quad A_{CP}^{mix}(B^0 \rightarrow \rho^0 \eta) \approx +25\%, \quad (95)$$

$$A_{CP}^{dir}(B^0 \rightarrow \rho^0 \eta') \approx -27\%, \quad A_{CP}^{mix}(B^0 \rightarrow \rho^0 \eta') \approx +11\%, \quad (96)$$

for  $\alpha \approx 100^\circ$ . For  $B^\pm \rightarrow \rho^\pm \eta$  decay, the CP-violating asymmetry around  $-15\%$  could be measured in the running B factory experiments. For the neutral decays, their CP-violating asymmetries may be measured in the forthcoming LHCb experiments.

- The major theoretical errors of the computed observables are induced by the uncertainties of the hard energy scale  $t_j$ 's, the parameters  $\omega_b$  and  $m_0^\pi$ , as well as the CKM angle  $\alpha$ .
- From the good consistency of the PQCD prediction of  $Br(B^+ \rightarrow \rho^+ \eta')$  with the measured value, we believe that the gluonic admixture of  $\eta'$  should be small, and most possibly not as important as expected before.

## Acknowledgments

We are very grateful to Li Ying for helpful discussions. This work is partly supported by the National Natural Science Foundation of China under Grant No.90103013, 10135060, 10275035, 10475085, 10575052, and by the Research Foundations of Jiangsu Education Committee and Nanjing Normal University under Grant No. 214080A916 and 2003102TSJB137.

## APPENDIX A: RELATED FUNCTIONS

We show here the function  $h_i$ 's, coming from the Fourier transformations of  $H^{(0)}$ ,

$$h_e(x_1, x_3, b_1, b_3) = K_0(\sqrt{x_1 x_3} m_B b_1) [\theta(b_1 - b_3) K_0(\sqrt{x_3} m_B b_1) I_0(\sqrt{x_3} m_B b_3) + \theta(b_3 - b_1) K_0(\sqrt{x_3} m_B b_3) I_0(\sqrt{x_3} m_B b_1)] S_t(x_3), \quad (A1)$$

$$h_a(x_2, x_3, b_2, b_3) = K_0(i\sqrt{x_2 x_3} m_B b_3) [\theta(b_3 - b_2) K_0(i\sqrt{x_3} m_B b_3) I_0(i\sqrt{x_3} m_B b_2) + \theta(b_2 - b_3) K_0(i\sqrt{x_3} m_B b_2) I_0(i\sqrt{x_3} m_B b_3)] S_t(x_3), \quad (A2)$$

$$h_f(x_1, x_2, x_3, b_1, b_2) = \left\{ \theta(b_2 - b_1) I_0(M_B \sqrt{x_1 x_3} b_1) K_0(M_B \sqrt{x_1 x_3} b_2) + (b_1 \leftrightarrow b_2) \right\} \cdot \left( \begin{array}{ll} K_0(M_B F_{(1)} b_1), & \text{for } F_{(1)}^2 > 0 \\ \frac{\pi i}{2} H_0^{(1)}(M_B \sqrt{|F_{(1)}^2|} b_1), & \text{for } F_{(1)}^2 < 0 \end{array} \right), \quad (A3)$$

$$h_f^1(x_1, x_2, x_3, b_1, b_2) = \left\{ \theta(b_1 - b_2) K_0(i\sqrt{x_2 x_3} b_1 M_B) I_0(i\sqrt{x_2 x_3} b_2 M_B) + (b_1 \leftrightarrow b_2) \right\} \cdot \left( \begin{array}{ll} K_0(M_B F_{(2)} b_1), & \text{for } F_{(2)}^2 > 0 \\ \frac{\pi i}{2} H_0^{(1)}(M_B \sqrt{|F_{(2)}^2|} b_1), & \text{for } F_{(2)}^2 < 0 \end{array} \right), \quad (\text{A4})$$

$$h_f^2(x_1, x_2, x_3, b_1, b_2) = \left\{ \theta(b_1 - b_2) K_0(i\sqrt{x_2 x_3} b_1 M_B) I_0(i\sqrt{x_2 x_3} b_2 M_B) + (b_1 \leftrightarrow b_2) \right\} \cdot \frac{\pi i}{2} H_0^{(1)}(\sqrt{x_1 + x_2 + x_3 - x_1 x_3 - x_2 x_3} b_1 M_B), \quad (\text{A5})$$

where  $J_0$  is the Bessel function and  $K_0$ ,  $I_0$  are modified Bessel functions  $K_0(-ix) = -(\pi/2)Y_0(x) + i(\pi/2)J_0(x)$ , and  $F_{(j)}$ 's are defined by

$$F_{(1)}^2 = (x_1 - x_2)x_3, \quad (\text{A6})$$

$$F_{(2)}^2 = (x_1 - x_2)x_3. \quad (\text{A7})$$

The threshold resummation form factor  $S_t(x_i)$  is adopted from Ref.[23]

$$S_t(x) = \frac{2^{1+2c}\Gamma(3/2+c)}{\sqrt{\pi}\Gamma(1+c)}[x(1-x)]^c, \quad (\text{A8})$$

where the parameter  $c = 0.3$ . This function is normalized to unity.

The Sudakov factors used in the text are defined as

$$S_{ab}(t) = s\left(x_1 m_B/\sqrt{2}, b_1\right) + s\left(x_3 m_B/\sqrt{2}, b_3\right) + s\left((1-x_3)m_B/\sqrt{2}, b_3\right) - \frac{1}{\beta_1} \left[ \ln \frac{\ln(t/\Lambda)}{-\ln(b_1\Lambda)} + \ln \frac{\ln(t/\Lambda)}{-\ln(b_3\Lambda)} \right], \quad (\text{A9})$$

$$S_{cd}(t) = s\left(x_1 m_B/\sqrt{2}, b_1\right) + s\left(x_2 m_B/\sqrt{2}, b_2\right) + s\left((1-x_2)m_B/\sqrt{2}, b_2\right) + s\left(x_3 m_B/\sqrt{2}, b_1\right) + s\left((1-x_3)m_B/\sqrt{2}, b_1\right) - \frac{1}{\beta_1} \left[ 2 \ln \frac{\ln(t/\Lambda)}{-\ln(b_1\Lambda)} + \ln \frac{\ln(t/\Lambda)}{-\ln(b_2\Lambda)} \right], \quad (\text{A10})$$

$$S_{ef}(t) = s\left(x_1 m_B/\sqrt{2}, b_1\right) + s\left(x_2 m_B/\sqrt{2}, b_2\right) + s\left((1-x_2)m_B/\sqrt{2}, b_2\right) + s\left(x_3 m_B/\sqrt{2}, b_2\right) + s\left((1-x_3)m_B/\sqrt{2}, b_2\right) - \frac{1}{\beta_1} \left[ \ln \frac{\ln(t/\Lambda)}{-\ln(b_1\Lambda)} + 2 \ln \frac{\ln(t/\Lambda)}{-\ln(b_2\Lambda)} \right], \quad (\text{A11})$$

$$S_{gh}(t) = s\left(x_2 m_B/\sqrt{2}, b_1\right) + s\left(x_3 m_B/\sqrt{2}, b_2\right) + s\left((1-x_2)m_B/\sqrt{2}, b_1\right) + s\left((1-x_3)m_B/\sqrt{2}, b_2\right) - \frac{1}{\beta_1} \left[ \ln \frac{\ln(t/\Lambda)}{-\ln(b_1\Lambda)} + \ln \frac{\ln(t/\Lambda)}{-\ln(b_2\Lambda)} \right], \quad (\text{A12})$$

where the function  $s(q, b)$  are defined in the Appendix B of Ref. [9] and the hard energy scale  $t_j$ 's have been given in Eq. (35).

- 
- [1] M. Beneke, G. Buchalla, M. Neubert, and C.T. Sachrajda, Phys. Rev. Lett. **83**, 1914 (1999).
  - [2] M. Beneke and M. Neubert, Nucl. Phys. B **675**, 333 (2003).
  - [3] G.P. Lepage and S. Brodsky, Phys. Rev. D **22**, 2157 (1980); J. Potts and G. Sterman, Nucl. Phys. B **225**, 62 (1989).
  - [4] C.-H. V. Chang and H.-n. Li, Phys. Rev. D **55**, 5577 (1997); T.-W. Yeh and H.-n. Li, Phys. Rev. D **56**, 1615 (1997).
  - [5] H.-n. Li, Prog. Part. & Nucl. Phys. **51**, 85 (2003), and reference therein.
  - [6] S. Descotes-Genon and C.T. Sachrajda, Nucl. Phys. B **625**, 239 (2002); H.-n. Li, p360-364, Proceedings of International Conference on Flavor Physics, Zhang-Jia-Jie 2001, Flavor physics, hep-ph/0110365; Z.-T. Wei, M.-Z. Yang, Nucl. Phys. B **642**, 263-289 (2002); M. Beneke and T. Feldmann, Nucl. Phys. B **685**, 296 (2004).
  - [7] M. Beneke, G. Buchalla, M. Neubert, and C.T. Sachrajda, Nucl. Phys. B **591**, 313 (2000).
  - [8] D.S. Du, H.J. Gong, J.F. Sun, D.S. Yang, and G.H. Zhu, Phys. Rev. D **65**, 094025 (2002).
  - [9] C.-D. Lü, K. Ukai and M.-Z. Yang, Phys. Rev. D **63**, 074009 (2001).
  - [10] Y.-Y. Keum, H.-n. Li and A.I. Sanda, Phys. Lett. B **504**, 6 (2001); Phys. Rev. D **63**, 054008 (2001).
  - [11] H.-n. Li, Phys. Rev. D **64**, 014019 (2001); S. Mishima, Phys. Lett. B **521**, 252 (2001); C.-H. Chen, Y.-Y. Keum, and H.-n. Li, Phys. Rev. D **64**, 112002 (2001); A.I. Sanda and K. Ukai, Prog. Theor. Phys. **107**, 421 (2002); C.D. Lü, Eur. Phys. J. C **24**, 121 (2002); C.-H. Chen, Y.-Y. Keum, and H.-n. Li, Phys. Rev. D **66**, 054013 (2002); Y.-Y. Keum and A.I. Sanda, Phys. Rev. D **67**, 054009 (2003).
  - [12] Y.-Y. Keum, T. Kurimoto, H.-n. Li, C.D. Lü, and A.I. Sanda, Phys. Rev. D **69**, 094018 (2004); Y. Li and C.D. Lü, J. Phys. G **29**, 2115 (2003); C.D. Lü, Phys. Rev. D **68**, 097502 (2003); Y. Li, C.D. Lü, Z.J. Xiao, and X.Q. Yu, Phys. Rev. D **70**, 034009 (2004); Y. Li, C.D. Lü, and Z.J. Xiao, J. Phys. G **31**, 273 (2005); X.Q. Yu, Y. Li and C.D. Lü, Phys. Rev. D **71**, 074026 (2005); C.D. Lü, Y.L. Shen and J. Zhu, Eur. Phys. J. C **41**, 311 (2005); J. Zhu, Y.L. Shen and C.D. Lü, Phys. Rev. D **72**, 054015 (2005); and J. Phys. G **32**, 101 (2006); Y. Li and C.D. Lü, Commun. Theor. Phys. **44**, 659 (2005); and Phys. Rev. D **73**, 014024 (2006); C.D. Lü, M. Matsumori, A.I. Sanda, and M.Z. Yang, Phys. Rev. D **72**, 094005 (2005).
  - [13] H.S. Wang, X. Liu, Z.J. Xiao, L.B. Guo and C.D. Lü, Nucl. Phys. B **738**, 243 (2006).
  - [14] G. Buchalla, A.J. Buras, M.E. Lautenbacher, Rev. Mod. Phys. **68**, 1125 (1996).
  - [15] A. Ali, G. Kramer, and C.D. Lü, Phys. Rev. D **58**, 094009 (1998), *ibid* **59**, 014005 (1999); Y.-H. Chen, H.-Y. Cheng, B. Tseng, and K.-C. Yang, Phys. Rev. D **60**, 094014 (1999).
  - [16] BaBar Collaboration, B. Aubert *et al.*, Phys. Rev. D **70**, 032006 (2004); BaBar Collaboration, B. Aubert *et al.*, Phys. Rev. Lett. **95**, 131803 (2005).
  - [17] Belle Collaboration, P. Chang *et al.*, Phys. Rev. D **71**, 091106(R) (2005); K. Abe *et al.*, BELLE-CONF-0408, ICHEP04 11-0653, Aug. 2004.
  - [18] CLEO Collaboration, A. Gritsan, *et al.*, talk given at Lake Louis Winter Institute, Feb. 20-26, (2000).
  - [19] Heavy Flavor Averaging Group, <http://www.slac.stanford.edu/xorg/hfag>.
  - [20] H.-n. Li, Phys. Rev. D **66**, 094010 (2002).

- [21] H.-n. Li and B. Tseng, Phys. Rev. D **57**, 443, (1998).
- [22] A.G. Grozin and M. Neubert, Phys. Rev. D **55**, 272 (1997); M. Beneke and T. Feldmann, Nucl. Phys. B **592**, 3 (2001).
- [23] T. Kurimoto, H.-n. Li, and A.I. Sanda, Phys. Rev. D **65**, 014007 (2001); C.D. Lu and M.Z. Yang, Eur. Phys. J. C **28**, 515 (2003).
- [24] C.-h. Chen and H.-n. Li, Phys. Rev. D **63**, 014003 (2000).
- [25] P. Ball, V.M. Braun, Y. Koike, and K. Tanaka, Nucl. Phys. B **529**, 323 (1998)
- [26] C.D. Lü and M.Z. Yang, Eur. Phys. J. C **23**, 275 (2002)
- [27] Particle Data Group, S. Eidelman *et al.*, Phys. Lett. B **592**, 1 (2004).
- [28] E. Kou, Phys. Rev. D **63**, 054027 (2001).
- [29] E. Kou and A.I. Sanda, Phys. Lett. B **525**, 240 (2002).
- [30] J.L. Rosner, Phys. Rev. D **27**, 1101 (1983).
- [31] P. Ball, J. High Energy Phys. 9809, 005 (1998); *ibid* , 9901, 010 (1999).
- [32] T. Feldmann and P. Kroll, Eur. Phys. J. C **5**, 327 (1998)
- [33] V.M. Braun and I.E. Filyanov , Z. Phys. C **48**, 239 (1990); P. Ball, J. High Energy Phys. 01, 010 (1999).
- [34] P. Ball and V.M. Braun, Phys. Rev. D **58**, 094016 (1998).
- [35] J. Charles *et al.*, Eur. Phys. J. C **41**, 1 (2005).
- [36] UTfit Collaboration, M. Bona *et al.*, JHEP 0507 (2005) 028.
- [37] H.-n. Li, S. Mishima, A.I. Sanda, Phys. Rev. D **72**, 114005 (2005).